

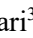




# Simultaneous Size, Shape and Topology Optimization of Truss Structures using the PSOSCALF Algorithm

Reza Najafi<sup>1\*</sup> , Ali Zabihi<sup>2</sup> , Reza Ansari<sup>3</sup> 

## ABSTRACT

The development of truss optimization approaches is one of the most essential structural engineering issues that recently attracts the attention of researchers. These approaches include size optimization, shape optimization, and topology optimization distinctly. In addition, the size, shape, and topology (SST) optimization is presented simultaneously. In previous researches, the choice of several different topologies was made individually to optimize the shape of the structure, which led to enhancing the computational cost and the time needed for the operation. Presented herein, a new optimization method of the SST optimization is introduced based on the PSOSCALF algorithm. The truss optimization procedure is started from a fixed initial configuration and, as it evolves, approaches its optimal shape. The considered constraints including stability, kinematics, tensile, and compression stresses in elements, and displacement in nodes, buckling for compression members that are used to optimize the SST of the 2D and 3D trusses. For evaluating, the outcomes are compared with the meta-heuristics algorithms presented in recent years such as Moth-Flame Optimization (MFO), Harris Hawks Optimization (HHO), Whale Optimization Algorithm (WOA), Water Cycle Algorithm (WCA), Teaching-Learning-Based Optimization (TLBO), Random learning mechanism-Particle Swarm Optimization-Levy Flight (RPSOLF), and Autonomous-Groups-Particles Swarm Optimization (AGPSO). The outcomes verify the supremacy of the PSOSCALF-based truss optimization in comparison with the mentioned algorithms.

**Keywords:** Size, Shape, and Topology Truss Optimization; Single Objective Optimization; Static Constraints; Meta-Heuristic Algorithms; PSOSCALF Algorithm.

## 1 Introduction

Nowadays, truss structures are widely employed in industrial applications due to their unique features, including a high strength-to-weight ratio, material efficiency, and ease of fabrication. They are extensively used in bridges, towers, aircraft, and spacecraft, where weight reduction and structural integrity are critical. In recent years, the optimization of truss structures has been an active research area, focusing on minimizing weight, maximizing strength, and improving overall efficiency. Researchers have explored various optimization techniques, such as size, shape, and topology optimization, to

---

<sup>1</sup> Department of Mechanical Engineering, Ahrar Institute of Technology & Higher Education, Rasht, Iran

\* Corresponding Author's email: [Rezanajafi93sas@gmail.com](mailto:Rezanajafi93sas@gmail.com)

<sup>2</sup> Department of Mechanical Engineering, Rowan University, 201 Mullica Hill Rd., Glassboro, NJ 08028, USA

<sup>3</sup> Department of Mechanical Engineering, University of Guilan, P.O. Box 3756, Rasht, Iran [r\\_ansari@guilan.ac.ir](mailto:r_ansari@guilan.ac.ir)

develop lightweight and cost-effective truss structures that meet engineering and industrial requirements.

In many engineering issues, the goal is to minimize the construction expense and the structural weight or to maximize the profits. In truss optimization topics, the objective function is usually introduced as the relationship between building value, the maximum displacement, and weight of the structure with different shape parameters called design variables. Design variables can include the cross-section of the members, coordinates of nodes, and how to connect the members of the truss. On the other hand, design variables are divided into two categories of continuous and discrete design variables, in which the continuous design variables are defined as the variables whose values change continuously, and they can take any amount in the design space. In contrast, the discrete design variables cannot have any value, and their value is chosen from predetermined set values. Besides this function, a series of criteria and limitations are considered for the problem called the problem constraints. These constraints may include structural stability, the kinematic of the structure, stress constraints in the members, displacement in the structural nodes, buckling in the elements, and the natural frequency of the structure [1].

Generally, the optimization of truss structures divided into four general classes such as optimization of size, shape, topology, and layout. Size optimization is the simplest type of truss optimization. In this branch of optimization, the main idea is to obtain the optimum cross-sectional areas of truss members assuming that the number of nodes and topology is constant. In these issues, the entire cross-sections of the structural members taken into account as design variables. Therefore, the computational cost is increased and the optimum solutions may be trapped in a local minimum. In shape optimization, the truss node coordinates are considered as design variables. In this branch of optimization, the shape of the structure in the optimization process constantly changed. The variables in the shape optimization procedure are the continuous values, and each value can be changed in the allowed interval. One of the most essential branches of optimization is topology optimization. In optimizing shape and size, since the connection of members with each other is known from the beginning, it is not possible to reduce the weight of the structure very effectively. In topology, the member's layout is one of the goals which is achieved during solving the structural optimization. This advantage can decrease the weight and the construction cost of the structure significantly. In the layout optimization, besides the size and topology variables, the geometry parameters of truss such as the coordinates of nodes are considered. The coordinates of the nodes are considered as continuous design variables, but in most cases, the variables of size and topology are discrete design variables. On the other hand, considering the simultaneous size, shape and topology, the number of design variables is significantly increased, and the truss optimization problem is complicated. However, applying this hybrid approach can have a favorable effect on the results of structural optimization [2].

Kaveh and Talatahar [3] combined the particle group algorithm with the ant colony technique and the harmonic search technique to optimize the size of truss structures with discrete and continuous variables. The modified teaching-learning based optimization algorithm was applied by Camp and Farshchin [4] to optimize truss. The size optimization of truss structures is analyzed with the help of continuous variables via artificial coronary circulation by Kooshkbaghi and Kaveh [5]. Cheng et al. [6] utilized the discrete variables and new variants of the harmony search algorithm to optimize trusses. Assim et al. [7] applied the genetic programming for topology and size optimization of truss structures. YueWu et al. [8] proposed the improved firefly algorithm with discrete variables for topology and size optimization of truss structures. Kaveh and Khalatjari [9] used the force method, genetic algorithm and graph theory

for topology and size optimization of truss structures. Ho-Huu et al. [10] employed discrete variables to improved constrained differential evolution using (D-ICDE) for layout optimization of truss structures. For layout optimization of truss structures, Ahrari and Deb [11] suggested an improved fully stressed design evolution strategy. The size and shape optimization of truss structures analyzed with help fully stressed design evolution strategy by Ahrari and Atai [12]. Mortazavi and Toğan [13] applied a modified particle swarm optimization algorithm for simultaneous SST optimization of trusses simultaneously. Ahrari et al. [14] combined the effect of SST optimization of truss structures by fully stressed design based on the evolution strategy. Miguel et al. [15] applied the firefly algorithm for a modified multimodal size, shape, and topology optimization of truss structures. Degertekin et al. [16] introduced the advanced Jaya algorithm for SST optimization of truss structures with discrete variables.

This article concerned with presented a simultaneous SST of six distinct 2D and 3D trusses using the PSOSCALF algorithm that is suggested in Ref. [17]. The outcomes of this study are compared with the seven meta-heuristics algorithms such as MFO, HHO, WOA, WCA, TLBO, RPSOLF and AGPSO. The stress, displacement, and kinematic stability as constraints and weight of the structure is considered as the objective function.

Most meta-heuristic methods have two significant problems, like the primary convergence behavior and trapping in the local optimum. Hence, the use of these methods in solving the optimization problem of different truss structures may not lead to the appropriate outcome. The gist of this article is to use a robust optimization algorithm to prevent these problems from occurring. Hence, in this paper, the developed prescription of the PSO algorithm is used to achieve high-quality responses. This algorithm called PSOSCALF and is introduced by Nezamivand Chegini et al. [17] in 2018. In the PSOSCALF algorithm, combined with particle swarm optimization (PSO), position updating equations in the sine cosine algorithm (SCA), algorithm and the Levy flight distribution. The sine and cosine functions behavior in the SCA algorithm ensures the exploitation and exploration capabilities in the optimization process. The Levy flight distribution generates various responses in the search space during the optimization procedure. Therefore, combining the equations of SCA and the distribution of Levy flight leads to a balance between the two phases of exploration and exploitation in the optimization process. The author in [17] has shown that the PSOSCALF algorithm in optimizing various benchmark functions and solving various engineering problems is superior to other PSO family algorithms and different meta-heuristic algorithms that have been published in recent years. Hence, in this paper, we use the PSOSCALF to optimize the 2D and 3D truss structures. Therefore, the results show that the PSOSCALF technique has a better performance in optimizing the structures than the MFO, HHO, WOA, WCA, TLBO, RPSOLF, AGPSO, algorithms.

The rest of this article is formed as follows: the meta-heuristic optimization algorithms used in this paper are briefly described in Section 2. In Section 3, the PSOSCALF algorithm is presented. The problem formulation and the results of the numerical examples are offered in Section 4 and 5, respectively. Consequently, the remarks are presented in the last section 6.

## 2 Meta-Heuristic Optimization Algorithms

The meta-heuristic algorithms inspired by the true behavior of the creatures in nature have gained momentum in recent years, and today they have many applications in different branches of science.

In these methods, unlike the precise optimization methods, near-optimal solutions are also met to a fair

level with an acceptable computational cost of searching and decision-makers

## 2.1 MFO Algorithm

Moth-Flame Optimization algorithm was proposed by Mirjalali [18] in which MFO is a nature-inspired meta-heuristic algorithm. In this optimizer, the butterfly navigation method which is called transverse orientation is the main inspiration. Butterflies fly at night for long distances, maintaining a constant angle concerning the moon. The deadly spiral path around artificial lights, and but these fantasy insects are trapped in a useless.

## 2.2 HHO Algorithm

The Harris Hawk's Optimization (HHO) was presented via Heidari et al. [19] in 2019. The main inspiration of the HHO is deduced from the cooperative behavior and pre-hunting style of the falconry group in nature by the surfing survey method. In this smart strategy, several hawks cooperate and attack in various ways, trying to surprise the prey.

## 2.3 WOA Algorithm

Mirjalili and Lewis [20] in 2016 proposed The Whale Optimization Algorithm (WOA). This algorithm is inspired by the social behavior of humpback whales in the hunting strategy.

## 2.4 WCA Algorithm

Water Cycle Algorithm (WCA) as an optimization method is introduced by Eskandar et al. [21] in 2012. The WCA is inspired through nature and based on the observation of the water cycle process and how rivers and streams flow to the sea in the real world.

## 2.5 TLBO Algorithm

Rao et al. [22] in 2011 presented firstly Teaching Learning Based Optimization (TLBO) algorithm. In the TLBO algorithm, a mathematical model for teaching and learning is considered. The TLBO method is implemented in two phases: the first phase is the teaching phase, and the second phase is the learning phase. One of the most prominent features of this algorithm is the lack of dependency on the parameters.

## 2.6 RPSOLF Algorithm

Bailu Yan et al. [23] in 2017 offered Random Learning Mechanism-Particle Swarm Optimization-Levy Flight (RPSOLF) algorithm. This algorithm is based on the specification of a random learning mechanism and Levy flight. The RPSOLF algorithm increments the diversity of the population by learning from stray particles and random walks in Levy flight.

## 2.7 AGPSO Algorithm

Mirjalali et al. [24] in 2014 presented firstly Autonomous-Groups-Particles Swarm Optimization (AGPSO) algorithm. The gist of this method is to increase the diversity of solutions in the search space using the concept of autonomous groups inspired by the variety of individuals in the original colonies.

### 3 The PSOSCALF Algorithm

The particle swarm optimization algorithm (PSO) is one of the population-based algorithms that has been widely used in many recent applications. Each of the members of the swarm called particle is determined by two vectors the position,  $\vec{X}_i(t)$ , and velocity,  $\vec{V}_i(t)$ , in the search space in the process of the optimization procedure. At the beginning of the optimization process, the particles with the position and velocity vectors are randomly generated in the design space. Then, in each replication of the implementation of the PSO algorithm, each particle moves in the search space based on its best personal experience,  $\vec{X}_{pBest}$ , and the best experience of the whole particles,  $\vec{X}_{gBest}$ . The updating equations of the position and velocity of each particle are as follows [25]:

$$\vec{V}_i(t+1) = w\vec{V}_i(t) + c_1r_1(\vec{X}_{pBest_i} - \vec{X}_i(t)) + c_2r_2(\vec{X}_{gBest} - \vec{X}_i(t)) \quad (1)$$

$$\vec{X}_i(t+1) = \vec{X}_i(t) + \vec{V}_i(t+1) \quad (2)$$

In the above relationships,  $\vec{V}_i(t+1)$  and  $\vec{X}_i(t+1)$  are the velocity vector and the position vector at the  $t+1$ -th moment, respectively. The parameters  $r_1$  and  $r_2$  are the random variables in the interval  $[0, 1]$ . The coefficients  $c_1$  and  $c_2$  are the personal learning factor and the global learning factor, respectively.  $w$  is the weighting factor that applies the effect of the previous velocity vector at the  $t$ -th instant in determining the new velocity vector at the  $t+1$ -th moment.

The PSO algorithm, in addition to its simplicity in implementation, has disadvantages such as the premature converging and falling at the local optimum. More recently, in 2018, Nezamivand Chegini et al. [17] presented the PSOSCALF approach for solving these issues. In the PSOSCALF algorithm, the position updating equations in the sine-cosine (SCA) optimization algorithm is combined with the Levy flight distribution. Then, by utilizing these hybrid relationships in the PSO technique, the exploration and exploitation phases are strengthened during the optimization process. Levy flight can create the long jump of the particles in the search space. This ability leads to a more effective search in the search space and producing the variant particles during the optimization process. The SCA algorithm transits smoothly from the exploration to exploitation using several random and adaptive variables and changing the range of the sine and cosine functions. Also, in this algorithm, the best approximation of global solution is saved in a variable called destination point and never disappeared during the optimization process. In the SCA method, the following relationships are used as the solution updating equations:

$$\vec{X}_i(t+1) = \begin{cases} \vec{X}_i(t) + z_1 \sin(z_2) |z_3 P^t - \vec{X}_i(t)|, & z_4 < 0.5 \\ \vec{X}_i(t) + z_1 \cos(z_2) |z_3 P^t - \vec{X}_i(t)|, & z_4 \geq 0.5 \end{cases} \quad (3a)$$

$$(3b)$$

where the parameters  $z_1, z_2, z_3$ , and  $z_4$  are the critical parameters of the SCA method.  $P^t$  is the destination point or the best solution obtained at time  $t$ . In PSOSCALF, the following combinational equations that have both benefits of the Levy flight and the SCA algorithms are used for producing the new responses:

$$\vec{X}_i(t+1) = \begin{cases} Levy_{walk}(\vec{X}_i(t)) + z_1 \sin(z_2) |z_3 \vec{X}_{gBest} - \vec{X}_i(t)|, & z_4 < 0.5 \\ Levy_{walk}(\vec{X}_i(t)) + z_1 \cos(z_2) |z_3 \vec{X}_{gBest} - \vec{X}_i(t)|, & z_4 \geq 0.5 \end{cases} \quad (4a)$$

$$(4b)$$

The difference between Eq. (4) in PSOSCALF and Eq. (3) SCA is in the expression of  $Levy_{walk}(\vec{X}_i(t))$ . This expression is calculated as follows [25]:

$$Levy_{walk}(\vec{X}_i(t)) = \vec{X}_i(t) + \overrightarrow{step} \oplus \overrightarrow{random}(size(\vec{X}_i(t))) \quad (5)$$

$$\overrightarrow{step} = stepsize \oplus \vec{X}_i(t)$$

In the PSOSCALF approach, the relationships presented in Eqs. (4a) and (4b) are added to the process of producing the new position of particles. In PSOSCALF, the number of times that the position of a particle does not change during the optimization process is stored in a parameter called the limit value. If this value is greater than or equal to the predetermined value, the position of the particle is calculated by the hybrid relationships in Eqs. (4a) and (4b).

The pseudo-code and flowchart of the PSOSCALF technique are shown in Fig. 1 and Fig. 2, respectively. At first, the population number,  $n_{pop}$ , the maximum iteration,  $MaxIt$  and search space range,  $X \in [X_{min}, X_{max}]$ , is determined. Then, the particles with an initial velocity and position vectors are produced, and  $\vec{X}_{pBest_i}$  and  $\vec{X}_{gBest}$  are specified using calculating the objective function in these particles and evaluating their fitness value. At each iteration of the PSOSCALF implementation, the limit value of each particle is investigated. If this value is less than the predetermined value, the particle is updated with the help of the original PSO relationships, i.e., Eqs. (1) and (2). Otherwise, the position of particle is obtained by the hybrid Eq. (4). In the next step, the objective function of each particle is calculated. The personal best experience,  $\vec{X}_{pBest_i}$ , and the global best experience,  $\vec{X}_{gBest}$ , are updated by comparing the new position of the particle with its previous positions and the positions of whole particles, respectively. If  $\vec{X}_{pBest_i}$  is improved, the controlling index of particle is reset to zero, and otherwise, the value of this index is increased by one unit. Finally,  $\vec{X}_{gBest}$  obtained at last iteration i.e.  $MaxIt$  is considered as the leading optimal solution.

#### 4 Problem Formulation

The general formulation of the truss structures for the SST optimization truss structures with continuous and discrete variables are presented as follows [26]:

$$\begin{aligned} \text{Find } X &= \{A_1, A_2, \dots, A_m, \xi_1, \xi_2, \dots, \xi_n\} && \text{Design variables} \\ \text{Minimize } f(A) &= \sum \rho_i A_i L_i && \text{Objective function} \\ \text{Subject to } G1 &= \text{Structure is suitable} && \\ G2 &= \text{Structure is kinematically stable} && \\ G3 &= \delta_{min} \leq \delta_i(A_i, \zeta) \leq \delta_{max} && j=1,2,\dots,n \\ G4 &= \sigma_{min} \leq \sigma_i(A_i, \zeta) \leq \sigma_{max}^{cr} && i=1,2,\dots,m \text{ for compression} \end{aligned} \quad (6)$$

$$\begin{aligned}
 G5 &= \sigma_{min} \leq \sigma_i(A_i, \xi) \leq \sigma_{max} & i=1,2,\dots,m \text{ for tension} \\
 G6 &= \sigma_i^b \leq \delta_i(A_i, \xi) \leq 0 & i=1,2,\dots,nc \\
 G7 &= A_i \in S = [0, A_1, \dots, A_{N_s}] & i=1,2,\dots,m \\
 G8 &= \xi_i^{min} \leq \xi_i \leq \xi_i^{max}
 \end{aligned}$$

---

```

Initialize the parameters (npop, MaxIt, Xmin, Xmax, dim)
trial (keeps the limit value for each particles) = 0
Initialize the particles with random positions (Xi) and random velocity (Vi) within initialization range in the
problem space
Evaluate the fitness
Set Xi to be XpBest
Set the particle with best fitness to be XgBest
for t = 1:MaxIt
    Calculation of c1(t), c2(t) and w(t)
    for i = 1:npop
        if trial(i)<limit
            Update the velocity Vi of particle using Eq. (1)
            Update the position Xi of particle using Eq. (2)
        else
            if rand() < 0.5
                Update the position Xi of particle using Eq. (4)
            else
                Update the position Xi of particle using Eq. (5)
            end if
        end if
        Position's value is brought to the boundary value when its value is moved out of the boundary in search
        space
        Evaluate fitness value for new particle Xi
        if f(Xi(t)) < f(XpBest)
            trial(i) = 0
            XpBest = Xi
        else
            Trial(i) = trial(i)+1;
        end if
        if f(XpBest) < f(XgBest)
            XgBest = XpBest
        end if
    end for
end for
    
```

---

**Fig. 1** Pseudo code of the PSOSCALF algorithm [17]

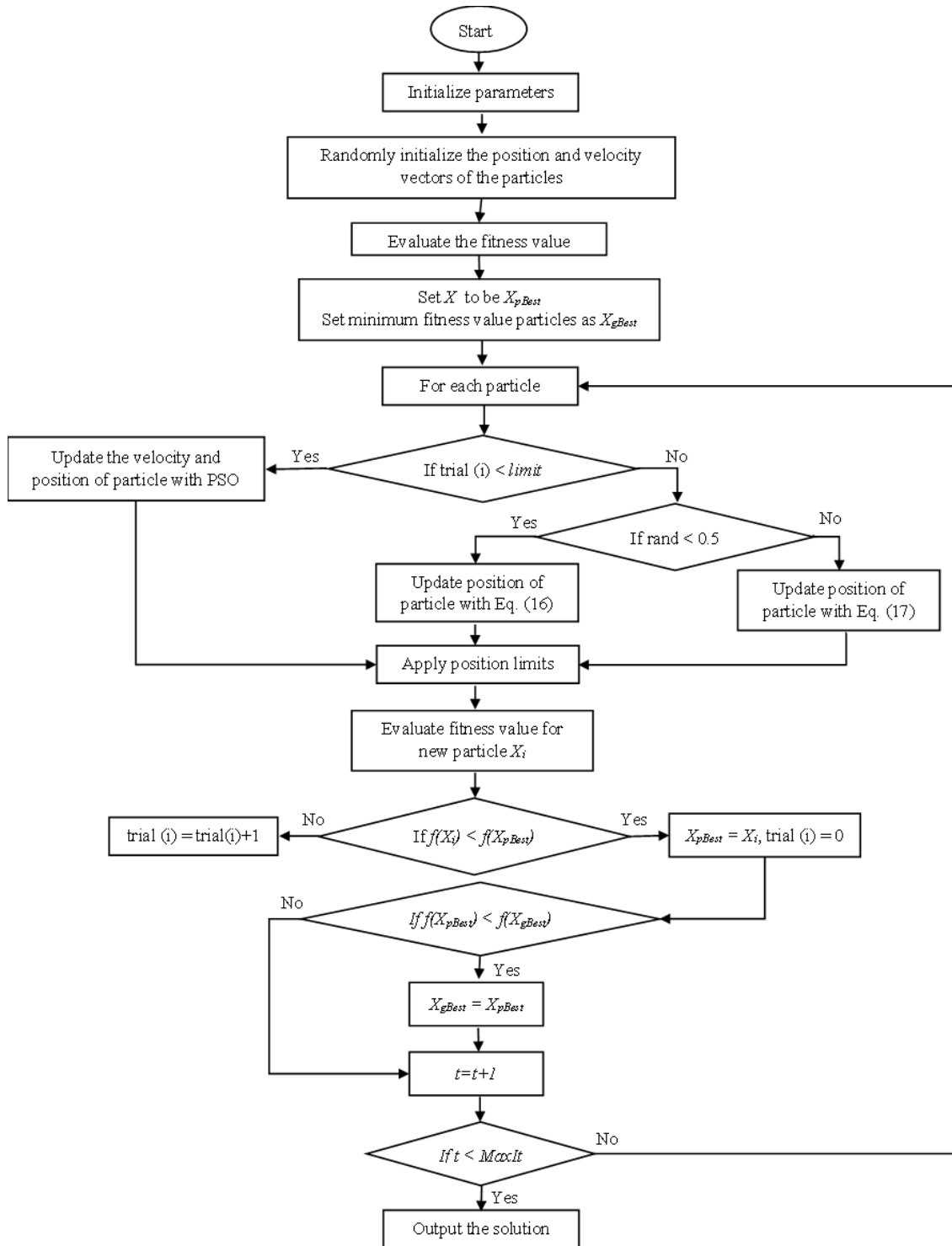


**Fig. 2** Flowchart of the PSOSCALF approach [17]

where  $f(A)$  is the weight of the structure,  $\rho_i$  is the density,  $A_i$ , is the cross-section areas and  $L_i$ , the length of the  $i^{th}$  member,  $m$  is the number of members.  $n$  is the number of truss nodes and,  $nc$  is the number of compression members.  $\delta_i$  and  $\delta_{max}$  respectively show the existing and permissible displacements for the node number  $j^{th}$  node, and  $\xi_i$  are coordinates of the node  $j^{th}$ .  $\sigma_i$  is the current stress in the  $i^{th}$  element, and  $\sigma_{max}$ ,  $\sigma_{max}^{cr}$  signify the permissible tensile and compression for the

$i^{th}$  element, respectively.  $\sigma_i^b$  demonstrates permissible buckling stress in  $i^{th}$  element when it is in compression. According to the above relations, the acronyms max and min implicate minimum and maximum allowable values, respectively.

The fitness function of a solution is dependent on the constraint violations and thus calculated as follows [26]:

$$f_{penalty}(X) = \begin{cases} 10^{15} & \text{if G1 is violated} \\ 10^{14} & \text{if G2 is violated with ID constraint} \\ 10^{13} & \text{if G2 is violated in the second step} \\ f(A) + 10^5 * \sum (|g_3(X)|) + \sum (|g_4(X)|) + \sum (|g_5(X)|) & \end{cases} \quad (7)$$

**Constraint G1.** In optimal truss design, some nodes are essential and should be available in every acceptable answer. These important nodes are usually loaded nodes and support nodes. These nodes are called main nodes (Deb and Gulati [26]). Thus, the central nodes must be in the structure and cannot be removed from it. This constraint is the main reason for the truss to be accepted. Therefore, this condition is initially controlled, and if one of the nodes is removed, a hefty fixed penalty is assigned to the solution, and no further calculation is done.

**Constraint G2:** In the optimization process, the PSOSCALF algorithm creates trusses with different topologies. Some of these trusses may not be kinematically stable. In this paper, the topological instability is detected before analysis structural, and in case of uncertainty, the particle is severely penalized. This process also ensures optimum stability of topological structures, significantly reduces the volume of arithmetic operations, and increases the speed of the algorithm. For this purpose, firstly, the degree of the static indeterminacy is determined using Eqs. (8) and (9) before the structural analysis operation is begun. If the degree of static indeterminacy is zero, the truss structure is a determinate statically. On the other hand, if the degree of static indeterminacy greater than zero, the truss structure is indeterminate statically. Finally, if the degree of static indeterminacy is negative, the corresponding structure is unstable, and a similar particle is fined. Therefore, in order not to be an unstable truss, its degree of static indeterminacy should be non-negative. The degree of static indeterminacy of truss for 2D and 3D models can be calculated using the following relationships [26]:

$$ID=m + r - 2 \times n \geq 0 \quad \text{in 2D model} \quad (8)$$

$$ID=m + r - 3 \times n \geq 0 \quad \text{in 3D model} \quad (9)$$

Where the number of nodes and members of truss in the structure is identified by n and m and degree of freedoms eliminated in the support nodes and, ID is the degree of static indeterminacy of truss.

**Constraints G3, G4 and G5:** If all the above conditions are met and the truss is not penalized, it will be analyzed. As noted earlier, because in the optimization process, trusses with different topologies are generated, and some of them may be statically determined and, some may be indeterminate. Therefore,

the finite element method (FEM) is used to calculate stresses and displacement. All truss members should have tensions within the limits of permissible resistance. Since the structure is usually exposed to several different loading modes separately, these constraints should be used for each loading mode. Also, the deformation resulting from the forces applied to all nodes (main and non-main) in the truss should not exceed the limit. To equalize the effect of constraints, all constraints are normalized by Eqs. (10) and (11) so that the violation of all constraints yields an equal value [26]:

$$S_i = \left| \frac{\sigma_i(A_i, \xi)}{\sigma_j^{max}} \right| - 1 \quad (10)$$

$$\delta_i = \left| \frac{\delta_i(A_i, \xi)}{\delta_j^{max}} \right| - 1 \quad (11)$$

$S_i$  and  $\delta_i$  are normalized tension and displacement, respectively. All of these standardized constraints must be smaller than zero, otherwise, depending on the amount of constraint violation, the penalty is added to the objective function.

**Constraint G6.** When a truss member is exposed to the compressive stress, it may fail if it exceeds its critical buckling load which is computed as follows [26]:

$$\sigma_i^{cr} = -\frac{KEA_i}{L_i^2} \quad (12)$$

where  $E$  signifies the modulus of elasticity, and  $k$  is the buckling ratio.

**Constraint G7:**  $A_i$  is selected from a discontinuous set of available sections, and  $S$  shows an acceptable set of  $A_i$ . For example  $S = \{0, A_1\}$  indicates that the cross-section of an existing member only can take the specified value  $A_1$  and the cross-section of an inactive zero member. In general,  $S = \{0, A_1, \dots, A_{N_s}\}$  represents that  $A_i$  can be one of the predefined positive value  $A_1, \dots, A_{N_s}$  for an existing member and zero for a non-existent member.

**Constraint G8:**  $\xi_j$ ,  $\xi_j^{min}$ , and  $\xi_j^{max}$  are the coordinates of  $j^{th}$  node, the lower, and the upper limit of the  $j^{th}$  truss node, respectively. The vector contains the variables of the  $\xi = (\xi_1, \dots, \xi_n)^T$  group coordinates and,  $n$  is the number of node coordinate variables. It is noted that the vector  $\xi$  contains the two-direction coordinates in the  $2D$  truss and the three-directions for the  $3D$  truss.

## 5 Numerical Examples

Herein, for evaluating the results of this study and investigate the capabilities of PSOSCALF, several usual structures are used. These examples have been widely used in various researches. In this study, six structures have been used. From these six structures, the structures of 10-bar  $2D$ , 15-bar  $2D$ , 18-bar  $2D$ , and 25-bar  $3D$  are utilized for simultaneous SST optimization with discrete variables, and 72-bar truss is used to simultaneous size and shape optimization with discrete variables. For appraising the

performance of the PSOSCALF algorithm in large structures, optimizing the truss-weight 120-bar dome with continuous design variables is investigated. The numbers of design variables for structures of 10, 15, 18, 25, 72, and 120 bars are 13, 23, 12, 13, 16, and 7, respectively. Also, the number of population for all examples is considered as 100. Also, for structures of 10, 15, 18, 25, 72, and 120 bars, the maximum number of iterations is regarded as 5000, 5000, 5000, 5000, 1000, and 500, respectively. The results of solving these problems with PSOSCALF algorithm are compared with other algorithms such as MFO, HHO, WOA, WCA, TLBO, RPSOLF, and AGPSO. In this section, the 30 runs are done and, the optimal result is obtained with the help of PSOSCALF algorithm. The PSOSCALF algorithm considers seven parameters as the minimum personal learning factor  $C_{1\ min}=0.5$ , the maximum personal learning factor  $C_{1\ max}=2.5$ , the minimum global learning factor  $C_{2\ min}=0.5$ , the maximum global learning factor  $C_{2\ max}=2.5$ , the minimum value of inertia weight  $W_{min}=0.4$ , and the maximum value of inertia weight  $W_{max}=0.9$ , the constant number that demonstrates the declining intensity of the weight factor  $K=10$ .

The PSOSCALF algorithm and problem formulation and finite element analysis of truss structures are coded in MATLAB software. The example results are executed on a laptop, having processor: Core i7 @ 2.40 GHz and installed memory 12.0 GB.

### 5.1 The 10-Bar Truss Structure

The first problem is the SST optimization of a 10 member and six nodes 2D truss as shown in Fig. 3. The material density and modulus of elasticity are  $0.1\ lb/in^3$  and  $10000\ ksi$ , respectively. The permissible stress of each member in tension and compressive is  $\pm 25\ ksi$ . The permissible deflection in all nodes and each direction is  $2\ in$ . As shown in Fig. 3, a perpendicular load of  $100\ kips$  applied on nodes 2 and 4. The cross-sectional areas of truss members are considered as size variables. The sizing variables are selected from 32 discrete values of  $S = \{1.62, 1.80, 2.38, 2.62, 2.88, 3.09, 3.13, 3.38, 3.63, 3.84, 3.87, 4.18, 4.49, 4.80, 4.97, 5.12, 5.74, 7.22, 7.97, 11.50, 13.50, 13.90, 14.20, 15.50, 16.00, 18.80, 19.90, 22.00, 22.90, 26.50, 30.00, 33.50\} in^2$ . In shape optimization, the  $y$ -coordinate of nodes 1, 3, and 5 are selected as shape variables and can vary between 180 and 1000  $in$  [13, 27]. In topology optimization, the presence or absence of truss members is selected as topology variables. To consider the topology, the value of zero is added to the set of existing cross-sections ( $S$ ). The information required to optimize this problem is presented in Table 1. The geometry of the truss after and before TSS optimization is shown in Fig. 4. Also, Fig. 5 shows the convergence curve behaviors of the best weight acquired via the optimization algorithms. As can be seen in Fig. 5, the PSOSCALF algorithm has shown better capability in two phases of exploration and exploitation than the other algorithms. The PSOSCALF evolution process is started at  $W \sim 7240.0179\ lb$  in the first iteration, converged to  $W \sim 2821.0317\ lb$  after 5000 iterations. The comparison of the existing value (the member's stresses are corresponding to the best solution) and allowable values for displacement constraints and stress are plotted in Fig. 6. According to the schemes, one can find that the displacement constraints and stress of the structure are not violated. Likewise, the presented optimum designs are thoroughly feasible. In this problem, the population size and maximum iteration are considered as 100 and 5000, respectively. The optimum best results obtained by the PSOSCALF and other algorithms are presented in Table 2. According to the result of the PSOSCALF algorithm in Table 2, elements 5 and 10 are removed from the base structure. The optimal weight for MFO, HHO, WOA, WCA, TLBO, RPSOLF, AGPSO and PSOSCALF algorithms are  $W \sim 3044.4911\ lb$ ,  $W \sim 2902.3278\ lb$ ,  $W \sim 3059.2871\ lb$ ,  $W \sim 3035.1288\ lb$ ,  $W \sim 2850.2401\ lb$ ,  $W \sim 2956.513\ lb$ ,  $W \sim 2856.6071\ lb$  and  $W \sim 2821.0317\ lb$ , respectively. In Table 2, the

outcomes among the methods and PSOSCALF is presented which verify the best design with the lowest cost.

**Table 1** Data for the 10-bar spatial truss problem

Design variables	Shape (3) Size (10)	$y_1; y_3; y_5$ $A_i, i=1,2,\dots,10$
Constraints	Stress Displacement Buckling	$(\sigma_c)_i \leq 172.4 \text{ MPa (25 ksi)}$ ; $(\sigma_t)_i \leq 172.4 \text{ MPa (25 ksi)}$ , $i=1,2,\dots,10$ $u_i \leq (2 \text{ in})$ None
Shape variables Area variables Size variables	$100 \text{ in} \leq y_1 \leq 180 \text{ in}$ ; $100 \text{ in} \leq y_3 \leq 180 \text{ in}$ ; $100 \text{ in} \leq y_5 \leq 180 \text{ in}$ ; $A_i \in S, i = 1, \dots, 10$ $S = \{1.62, 1.80, 2.38, 2.62, 2.88, 3.09, 3.13, 3.38, 3.63, 3.84, 3.87, 4.18, 4.49, 4.80, 4.97, 5.12, 5.74, 7.22, 7.97, 11.50, 13.50, 13.90, 14.20, 15.50, 16.00, 18.80, 19.90, 22.00, 22.90, 26.50, 30.00, 33.50\} (\text{in}^2)$ .	
Loading	Nodes 2, 4	$F_x \text{ (Kips)}$ $F_y \text{ (Kips)}$ 0.0                      -100.0
Mechanical Properties	Modulus of elasticity: $E=1.0 \times 10^4 \text{ ksi}$ Density of the material: $\rho=0.1 \text{ lb/in}^3$	

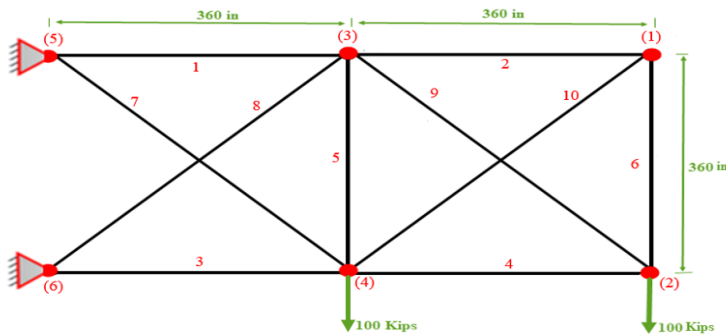


**Fig. 3** Base structure a 10-bar truss problem

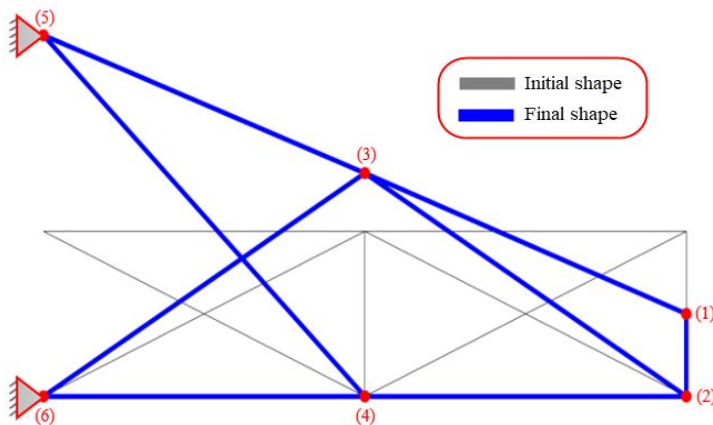


**Fig. 4** Optimized size, shape, and topology 10- bar truss obtained by PSOSCALF

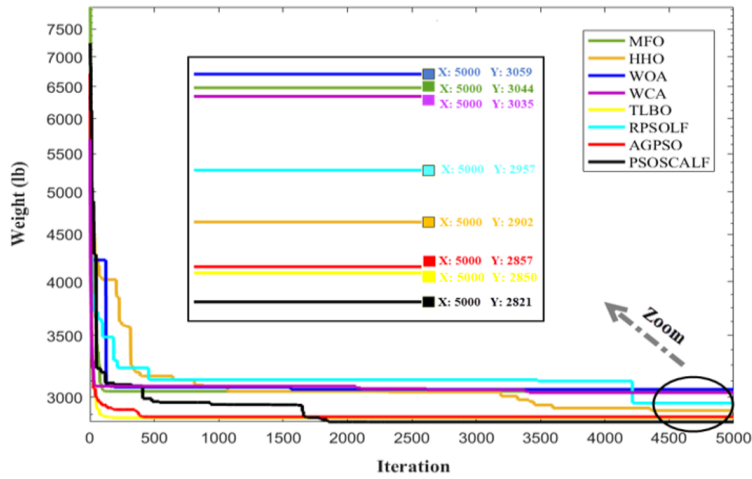


**Fig. 5** Convergence diagram for optimizing 10-bar truss Size, shape and topology (X= Max iteration, Y= Cost function)

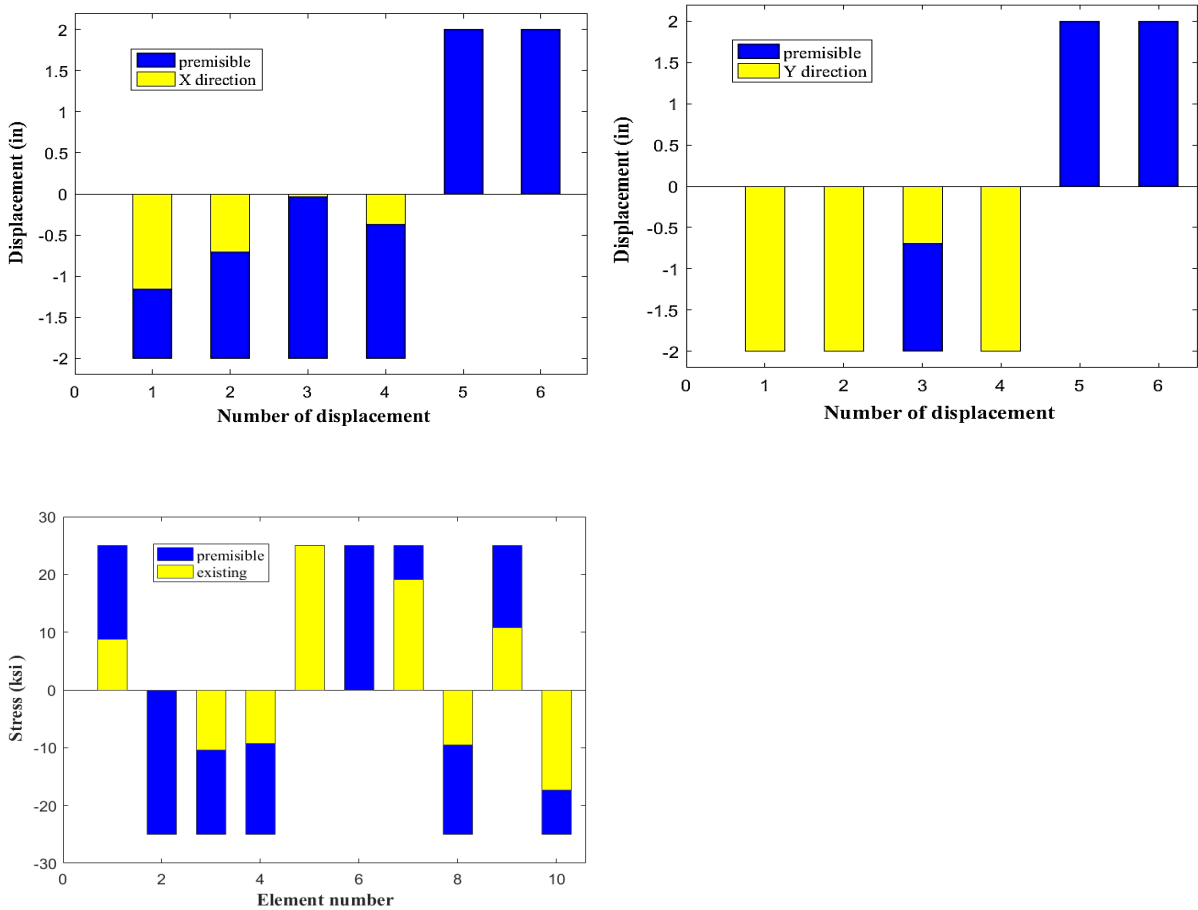


**Fig. 6** Comparison of existing and permissible stresses and displacements for the 10-bar truss by PSOSCALF, (a, b) Constraint values of displacement, (c) Constraint values of stress

**Table 2** Comparison of optimal designs for size, shape, and topology of the 10-bar truss

Design variables $A_i$ ( $in^2$ ) & $\xi_i$ ( $in$ )	MFO	HHO	WOA	WCA	TLBO	RPSOLF	AGPSO	PSOSCALF
$A_1$	15.5	14.2	11.5	18.8	13.5	16	13.5	<b>13.5</b>
$A_2$	1.62	1.62	2.38	1.62	1.62	1.8	1.62	<b>1.62</b>
$A_3$	7.97	11.5	11.8	11.5	7.97	11.5	7.97	<b>11.5</b>
$A_4$	7.97	7.97	5.12	11.5	7.22	7.97	7.97	<b>7.79</b>
$A_5$	Remove d	1.8	Remove d	4.97	1.62	1.8	1.62	<b>Removed</b>
$A_6$	1.62	1.62	1.62	1.62	1.62	1.62	1.62	<b>1.62</b>
$A_7$	7.97	3.63	5.74	Remove d	4.18	3.38	4.18	<b>5.74</b>
$A_8$	2.38	2.62	2.38	2.88	3.84	3.38	3.63	<b>3.09</b>
$A_9$	13.5	13.5	13.9	13.5	11.5	13.5	11.5	<b>11.5</b>
$A_{10}$	Remove d	1.62	Remove d	1.62	1.62	Remove d	1.62	<b>Removed</b>
Shape variables ( $in$ )								
$Y_5$	782.581	796.838	800.754	771.686	868.650	791.388	865.914	<b>787.9502</b>
	8	2	9	2	8	2	3	
$Y_3$	472.630	443.312	492.273	379.020	496.505	457.727	521.810	<b>487.0206</b>
	9	8	3	1	8	8	0	
$Y_1$	180	183.886	426.234	180	180	180	180	<b>180</b>
		2	9					
Weight ( $lb$ )	3044.49	2902.32	3059.28	3035.12	2850.24	2956.51	2856.60	<b>2821.0317</b>
	11	77	71	88	01	31	71	
Max.stress ( $ksi$ )	10.9237	15.6879	14.2832	22.6740	12.7303	15.9556	10.8780	<b>17.3837</b>
Max.displacement ( $in$ )	2.0000	2.0000	2.0000	2.0000	2.0000	1.9794	1.9996	<b>2.0000</b>

## 5.2 The 15-Bar Truss Structure

The second problem is a 15-bar and 8 nodes 2D truss structure illustrated in Fig.7. In this issue, the goal is to minimize the weight of the truss with stress constraints. The upright load of 10 kips is entered into node 8. The stress bound for all members in tension and compressive is  $\pm 25$  ksi. The material density and modulus of elasticity are  $0.1 \text{ lb/in}^3$  and 10000 ksi, respectively. The cross-sectional areas of truss members have been elected from 32 discrete amounts  $S = \{ 0.111, 0.141, 0.174, 0.220, 0.270, 0.287, 0.347, 0.440, 0.539, 0.954, 1.081, 1.174, 1.333, 1.488, 1.764, 2.142, 2.697, 2.800, 3.131, 3.565, 3.813, 4.805, 5.952, 6.572, 7.192, 8.525, 9.300, 10.850, 13.330, 14.290, 17.170, 19.180 \} in^2$ . In the shape optimization, the coordinates of nodes 2, 3, 6 and 7 are allowed to change in the  $x$  and  $y$ -directions. The  $x$ -coordinates of nodes 2 and 3 must be equal to the  $x$ -coordinates of nodes 6 and 7, respectively. The nodes 4 and 8 can only be changed in the  $y$ -direction. The layout issue of this truss includes 15 size variables and 8 variables of the form  $(x_2 = x_6, x_3 = x_7, y_2, y_3, y_4, y_6, y_7, y_8)$  [28, 29]. The lateral constraints and other optimization information for this truss are presented in Table 3. The geometry of the truss after and before TSS optimization is shown in Fig. 8. As can be seen, the coordinates of nodes 4 and 8 in the  $y$ -direction obtained by the PSOSCALF algorithm are very closely matched. Fig. 9 shows the comparison of convergence curves for MFO, HHO, WOA, WCA, TLBO, RPSOLF, AGPSO and PSOSCALF. The optimization results again show the superiority of the

PSOSCALF over the other algorithms. The PSOSCALF evolution process is started at  $W \sim 847.6390 \text{ lb}$  in the first iteration, then converged to  $W \sim 73.4761 \text{ lb}$  after 5000 iterations. The ratio of member's stress in the optimal result obtained by the PSOSCALF optimization algorithm is shown in Fig. 10. This illustration indicates that the optimal answer does not violate any of the primary constraints of the problem. In this section, it is regarded as the population size and the maximum iteration as 100 and 5000, respectively. Table 4 compares the optimum results attained from this work. From the results of PSOSCALF algorithm in Table 4, we can see that the elements 7 and 8 are removed from the base structure. The results indicate that the MFO, HHO, WOA, WCA, TLBO, RPSOLF, AGPSO and PSOSCALF algorithms design optimum truss with a minimum weight of  $W \sim 110.0627 \text{ lb}$ ,  $W \sim 96.4409 \text{ lb}$ ,  $W \sim 99.7857 \text{ lb}$ ,  $W \sim 86.7491 \text{ lb}$ ,  $W \sim 79.3254 \text{ lb}$ ,  $W \sim 97.8706 \text{ lb}$ ,  $W \sim 75.8720 \text{ lb}$  and  $W \sim 73.4761 \text{ lb}$ , respectively. These results indicate the performance of the PSOSCALF method to solve this problem.

**Table 3** Data for the 15-bar spatial truss problem

Design variables	Shape (8) Size (15)	$x_2 = x_6; x_3 = x_7; y_2; y_3; y_4; y_6; y_7; y_8$ $A_i, i=1,2,\dots,15$
Constraints	Stress Displacement Buckling	$(\sigma_c)_i \leq 172.4 \text{ MPa (25 ksi)}$ ; $(\sigma_t)_i \leq 172.4 \text{ MPa (25 ksi)}$ , $i=1,2,\dots,15$ None None
Shape variables Area variables Size variables	$100 \text{ in} \leq x_2 \leq 140 \text{ in}; 50 \text{ in} \leq y_4 \leq 90 \text{ in}; 220 \text{ in} \leq x_3 \leq 260 \text{ in}; -20 \text{ in} \leq y_6 \leq 20 \text{ in}$ $100 \text{ in} \leq y_2 \leq 140 \text{ in}; -20 \text{ in} \leq y_7 \leq 20 \text{ in}; 100 \text{ in} \leq y_3 \leq 140 \text{ in}; 20 \text{ in} \leq y_8 \leq 60 \text{ in}$ $A_i \in S, i = 1, \dots, 15$ $S = \{0.111, 0.141, 0.174, 0.22, 0.27, 0.287, 0.347, 0.44, 0.539, 0.954, 1.081, 1.174, 1.333, 1.488, 1.764, 2.142, 2.697, 2.8, 3.131, 3.565, 3.813, 4.805, 5.952, 6.572, 7.192, 8.525, 9.3, 10.85, 13.33, 14.29, 17.17, 19.18\} (\text{in}^2)$	
Loading	Nodes 8	$F_x \text{ (Kips)}$ 1.0 $F_y \text{ (Kips)}$ -10.0
Mechanical Properties	Modulus of easticity: $E=1.0 \times 10^4 \text{ ksi}$ Density of the material: $\rho=0.1 \text{ lb/in}^3$	

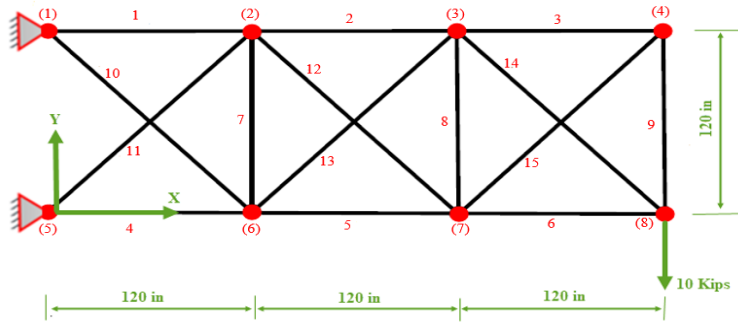


**Fig. 7** Base structure a 15-bar truss problem

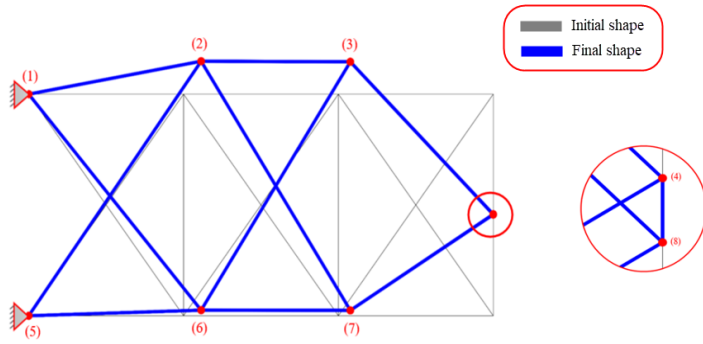


**Fig. 8** Optimized size, shape, and topology 10- bar truss obtained by PSOSCALF

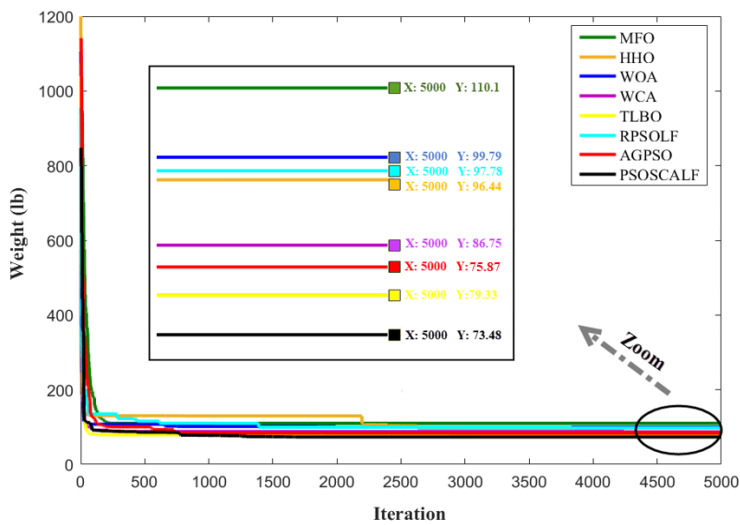


**Fig. 9** Convergence diagram for optimizing 15-bar truss Size, shape and topology (X= Max iteration, Y= Cost value)

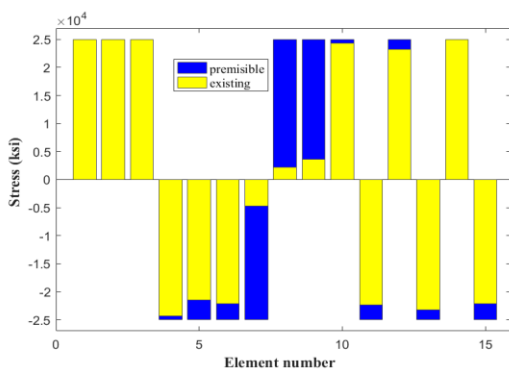


**Fig. 10** Comparison of existing and permissible stresses for the 15-bar truss by PSOSCALF

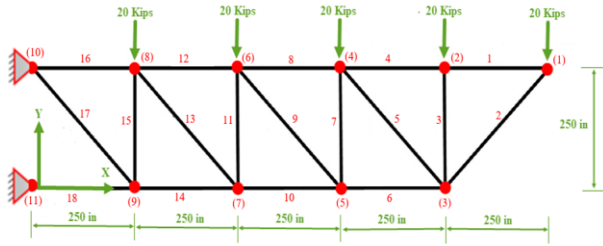


Fig. 11 Base structure a 18-bar truss problem

Table 4 Comparison of optimal designs for simultaneous size, shape, and topology of the 15-bar truss

Design variables $A_i$ ( $in^2$ ) & $\zeta_i$ (in)	MFO	HHO	WOA	WCA	TLBO	RPSOLF	AGPSO	PSOSCALF
$A_1$	1.3330	1.0810	0.9540	1.0810	1.1740	1.4880	0.9540	<b>0.9540</b>
$A_2$	0.5390	1.0810	0.9540	0.9540	0.9540	0.9540	0.9540	<b>0.5390</b>
$A_3$	0.9540	0.4400	0.4400	Removed	0.4400	0.4400	0.1110	<b>0.1410</b>
$A_4$	1.3330	0.9540	1.3330	1.0810	1.1740	1.0810	1.0810	<b>0.9540</b>
$A_5$	1.7640	0.9540	0.5390	0.5390	0.9540	1.3330	0.5390	<b>0.5390</b>
$A_6$	0.1110	0.4400	0.1110	0.9540	0.1440	0.2200	0.4400	<b>0.2700</b>
$A_7$	0.1110	0.4400	0.2700	Removed	Removed	0.2200	Removed	<b>Removed</b>
$A_8$	0.2700	0.1740	0.9540	0.1410	Removed	0.3470	0.1110	<b>Removed</b>
$A_9$	19.800	0.1740	0.3470	0.1110	0.3470	0.9540	0.1110	<b>0.9540</b>
$A_{10}$	0.1110	0.1740	0.9540	0.2700	0.1110	Removed	0.3470	<b>0.3470</b>
$A_{11}$	Removed	0.4400	Removed	0.2200	0.1110	0.2200	0.1740	<b>0.4400</b>
$A_{12}$	1.0810	0.1740	Removed	0.1110	0.4400	0.5390	Removed	<b>0.2200</b>
$A_{13}$	Removed	0.4400	0.9540	0.4400	0.3470	0.1740	0.5390	<b>0.3470</b>
$A_{14}$	Removed	0.4400	0.1110	0.9540	0.1410	0.3470	0.5390	<b>0.2700</b>
$A_{15}$	0.9540	0.2700	0.4400	0.1110	0.4400	0.4400	0.1110	<b>0.1410</b>
Shape variables (in)								
$X_2$	102.5716	120.3234	100	100	120.4280	100	116.9630	<b>133.6413</b>
$X_3$	260	200	242.7660	260	220	220	231.7665	<b>249.2493</b>
$Y_2$	100	120.0238	127.2853	120.5095	100	100	122.2930	<b>137.8416</b>
$Y_3$	106.3617	118.2851	100	100.0059	104.4972	100	107.5495	<b>137.5304</b>
$Y_4$	54.5346	70.9654	53.2716	50	53.1678	50	50	<b>54.9782</b>
$Y_6$	11.6676	5.0763	16.2830	7.4146	12.0347	1.2160	5.6653	<b>3.0316</b>
$Y_7$	20	5.1150	8.3821	12.2615	1.8373	2.0620	9.8754	<b>2.9063</b>
$Y_8$	54.5346	28.6857	53.2717	49.6610	53.1679	20	37.3784	<b>54.8021</b>
Weight (lb)	110.0627	96.4409	99.7857	86.7491	79.3254	97.8706	75.8720	<b>73.4761</b>
Max. stress (ksi)	25.0000	24.9997	24.8677	25.0000	25.0000	24.3500	25.0000	<b>24.2744</b>

### 5.3 The 18-Bar Truss Structure

Fig. 11 shows the geometry and loading conditions of the third example that has 18 members and 11 nodes. This structure is subjected to the concentrated load of 20 kips, which is applied to the upper truss nodes, according to Fig. 11. It is assumed that all members are made from a material with a modulus of elasticity of 10000 ksi and a density of 0.1 lb/in<sup>3</sup>. The stress limit for all members in tension and compressive is ±20 ksi. Also, buckling constraint is also intended for pressure members. The cross-sectional area of truss members is divided into 4 groups. The size design variables of the discrete set of 80 sections are selected from 2 in<sup>2</sup> to 21.75 in<sup>2</sup> with a step size of 0.25 in<sup>2</sup>. In the shape optimization, the position of nodes 3, 5, 7 and 9 can be changed in both directions x and y. The lateral constraints for shape variables are following Table 5. Truss characteristics are offered in Table 5 [30, 10]. The geometry of the truss after and before TSS optimization is shown in Fig. 12. The convergence behavior of the MFO, HHO, WOA, WCA, TLBO, RPSOLF, AGPSO and PSOSCALF applying on the 18-bar planar



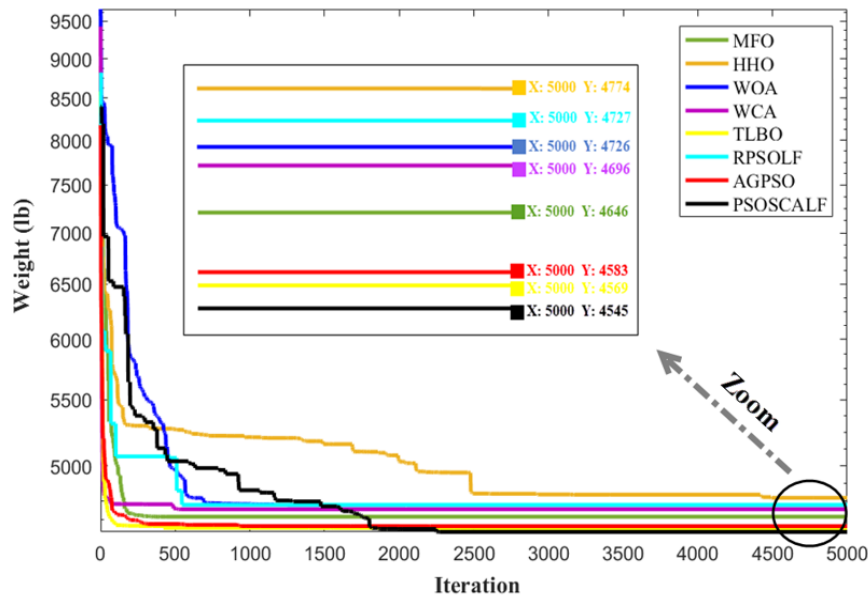


**Fig. 13** Convergence diagram for optimizing 18-bar truss Size, shape and topology (X= Max iteration, Y= Cost value)

**Table 6** Comparison of optimal designs for simulates size, shape, and topology of the 18-bar truss

Design variables $A_i$ ( $in^2$ ) & $\xi_i$ ( $in$ )	MFO	HHO	WOA	WCA	TLBO	RPSOLF	AGPSO	PSOSCALF
$A_1$	11.75	10	12.25	12.75	11.5	10.25	10.75	<b>12.5</b>
$A_2$	15.25	15.25	15	15.25	15.25	15.5	15.25	<b>15.25</b>
$A_3$	2.75	4	3.75	2.5	2	5.25	2	<b>3</b>
$A_5$	4.5	6	5.75	3.5	4.25	8.25	5.5	<b>3.5</b>
Shape variables ( $in$ )								
$X_3$	838.87	861.75	819.51	889.42	907.72	775	890.76	<b>826.81</b>
$Y_3$	525	595.92	583.82	598.96	602.35	525	600.62	<b>638.21</b>
$X_5$	385.74	325.86	448.87	406.93	365.44	275	387.08	<b>366.42</b>
$Y_5$	240.71	338.90	138.20	190.47	291.84	210.67	271.14	<b>228.15</b>
$X_7$	187.10	125.93	200.06	201.74	196.72	125.55	186.93	<b>188.70</b>
$Y_7$	128.72	107.89	147.98	155.63	135.29	19.16	125.11	<b>162.09</b>
$X_9$	83.44	29.43	110.85	103.15	72.76	113.23	68.45	<b>85.48</b>
$Y_9$	33.28	42.97	23.45	30.58	50.80	25.44	27.27	<b>41.23</b>
Weight ( $lb$ )	4646	4774.3462	4726.11	4696.37	4569.39	4727.13	4583.31	<b>4545.47</b>

#### 5.4. The 25-Bar Truss Structure

In this case, the fourth issue is considered by a 25 member and eight-node 3D truss shown in Fig. 15. According to Table 7, the cross-sectional area of truss members is divided into 8 groups to reduce the number of variables. Design variables are elected from 30 discrete values of  $S = \{0.1, 0.2, 0.3, 0.4, 0.5, 0.6, 0.7, 0.8, 0.9, 1.0, 1.1, 1.2, 1.3, 1.4, 1.5, 1.6, 1.7, 1.8, 1.9, 2.0, 2.1, 2.2, 2.3, 2.4, 2.5, 2.6, 2.8, 3.0, 3.2, 3.4\} in^2$ . The material density and modulus of elasticity are  $0.1 lb/in^3$  and  $10000 ksi$ , respectively. The stress permissible for each member in tension and compressive is  $\pm 40 ksi$ . The deflection permissible

in all nodes and each direction is 0.35 in. In shape optimization, the coordinates of nodes 3, 4, 5 and 6 can be changed in  $x$ ,  $y$  and  $z$  directions. Likewise, the coordinates of nodes 7, 8, 9, and 10 are allowed to change in the  $x$  and  $y$  directions, while the positions of joints 1 and 2 remain unchanged. Given the symmetry of the problem, the  $x$ - $z$  and  $y$ - $z$  planes the shape variables are considered as  $x_4, y_4, z_4, x_8$  and  $y_8$ . The layout issue of this truss includes 8 size variables and 5 shape variables. The lateral constraints for shape variables and loading information truss and other optimization information for this truss are given in Table 8 [13]. In topology optimization, the presence or absence of truss members is selected as topology variables. The geometry of the truss after and before TSS optimization is shown in Fig 16. The PSOSCALF evolution process is started at  $W \sim 222.3496 \text{ lb}$  in the first iteration and converged to  $W \sim 115.9406 \text{ lb}$  after 5000 iterations. The convergence diagram of the best results as shown in Fig 17. The ratio of member's stress and nodes displacement in the optimal result obtained by PSOSCALF algorithm is shown in Fig 18. This figure indicates that the optimal answer does not violate any of the primary constraints of the problem. In this problem, the population size and the maximum iteration are considered as 100 and 5000, respectively. Table 9 compares the optimum results obtained from this work. According to the result of the PSOSCALF algorithm in Table 9, elements 10, 11, 12 and 13 are removed from the base structure. The optimal weights obtained by MFO, HHO, WOA, WCA, TLBO, RPSOLF, AGPSO and PSOSCALF algorithms are  $W \sim 121.94319 \text{ lb}$ ,  $W \sim 134.2295 \text{ lb}$ ,  $W \sim 133.2506 \text{ lb}$ ,  $W \sim 119.6150 \text{ lb}$ ,  $W \sim 118.0741 \text{ lb}$ ,  $W \sim 166.5620 \text{ lb}$ ,  $W \sim 116.7475 \text{ lb}$ ,  $W \sim 115.9406 \text{ lb}$ , respectively.

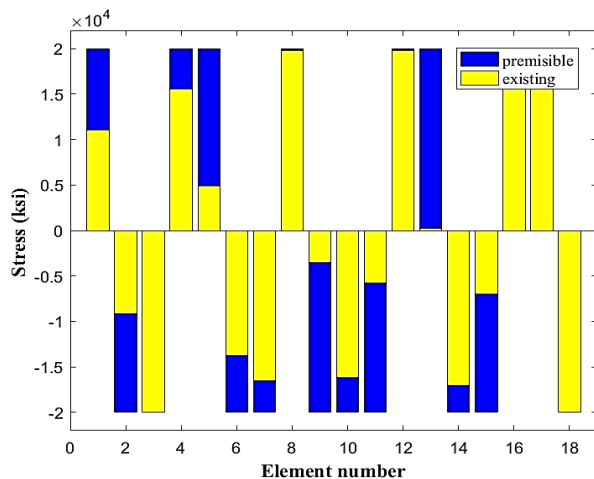


**Fig. 14** Comparison of existing permissible stresses for the 18-bar truss by PSOSCALF.

**Table 7** Member grouping for the 25-bar 3D truss.

Group	Members (end nodes)
$A_1$	1 (1,2)
$A_2$	2 (1,4), 3 (2,3), 4 (1,5), 5 (2,6)
$A_3$	6 (2,5), 7 (2,4), 8 (1,3), 9 (1,6)
$A_4$	10 (3,6), 11 (4,5)
$A_5$	12 (3,4), 13 (5,6)
$A_6$	14 (13,10), 15 (6,7), 16 (4,9), 17 (5,8)
$A_7$	18 (3,8), 19 (4,7), 20 (6,9), 21 (5,10)
$A_8$	22 (3,7), 23 (4,8), 24 (5,9), 25 (6,10)

**Table 8** Data for the 25-bar 3D truss problem.

Design variables	Shape (5) Size (8)	$x_4 = x_5 = -x_3 = -x_6$ ; $y_3 = y_4 = -y_5 = -y_6$ ; $z_3 = z_4 = z_5 = z_6$ ; $x_8 = x_9 = -x_7 = -x_{10}$ ; $y_7 = y_8 = -y_9 = -y_{10}$ ; $A_i, i=1,2,\dots,8$		
Constraints	Stress Displacement Buckling	$(\sigma_c)_i \leq 40 \text{ ksi}$ ; $(\sigma_t)_i \leq 40 \text{ ksi}$ , $i=1,2,\dots,25$ $u_i \leq 0.35 \text{ in}$ None		
Shape variables	$20 \text{ in} \leq x_4 \leq 60 \text{ in}$ $40 \text{ in} \leq x_8 \leq 80 \text{ in}$ $40 \text{ in} \leq y_4 \leq 80 \text{ in}$ $100 \text{ in} \leq y_8 \leq 140 \text{ in}$ ; $90 \text{ in} \leq z_4 \leq 130 \text{ in}$			
Area variables	$A_i \in S, i = 1, \dots, 25$			
Size variables	$S = \{0.1, 0.2, 0.3, \dots, 2.6\} \cup \{2.8, 3.0, 3.2, 3.4\} \text{ (in}^2\text{)}$			
Loading	Nodes	$F_x$ (Kips)	$F_y$ ( Kips )	$F_z$ (Kips)
	1	1.0	-10.0	-10.0
	2	0.0	-10.0	-10.0
	3	0.5	0.0	0.0
Mechanical Properties	Modulus of elasticity: $E= 1.0 \times 10^4 \text{ ksi}$ Density of the material: $\rho= 0.1 \text{ lb/in.}^3$			

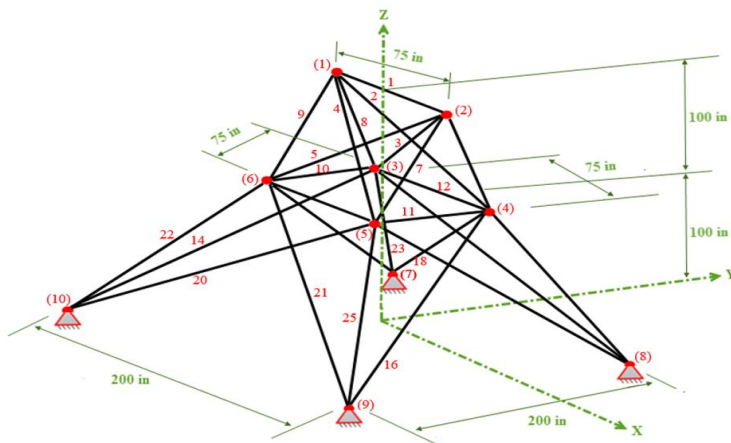


**Fig. 15** Base structure a 25-bar space truss problem.

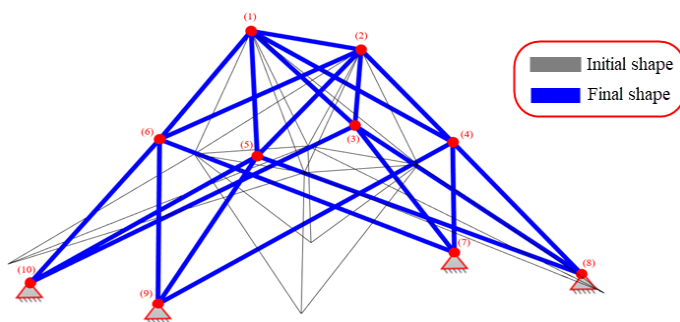


**Fig. 16** Optimized size, shape, and topology 25- bar truss obtained by PSOSCALF.

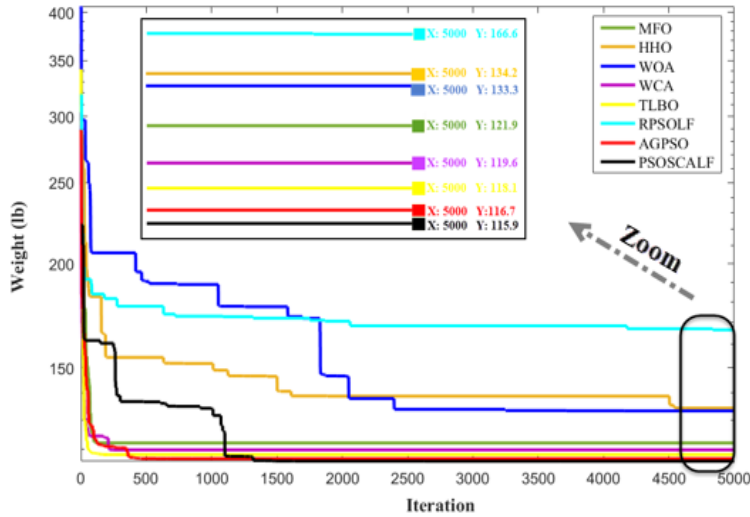


**Fig. 17** Convergence diagram for optimizing 25-bar space truss Size, shape and topology (X= Max iteration, Y= Cost value).

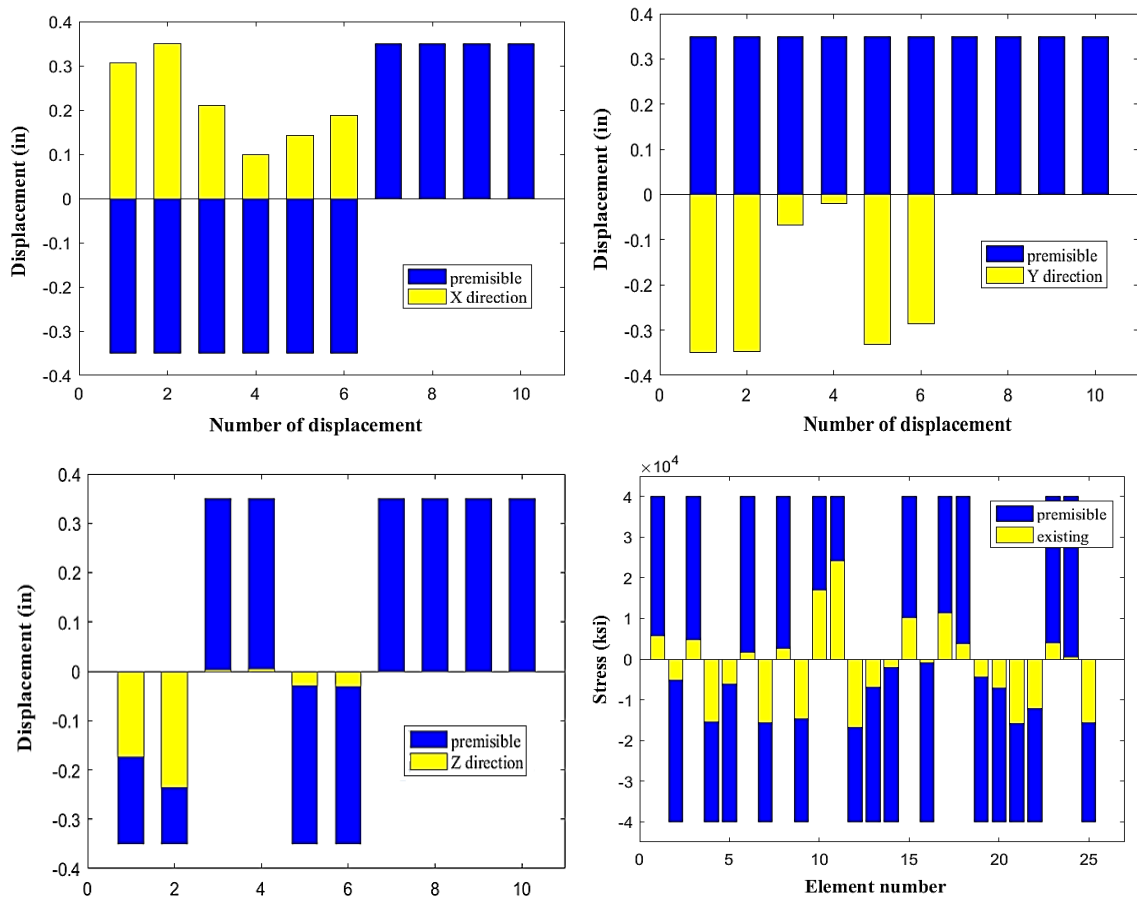


**Fig. 18** Comparison of existing and permissible stresses and displacements for the 10-bar truss by PSOSCALF, (a,b,c) Constraint values of displacement, (d) Constraint values of stress.

## 5.4 The 72-Bar Spatial Truss

The truss optimized in this subsection is the spatial 72 bars connected by 20 nodes as shown in Fig. 19. Which is considered as the fifth example to optimize size and topology. The material density and modulus of elasticity are  $0.1 \text{ lb/in}^3$  and  $10000 \text{ ksi}$  respectively. The elements are subjected to the stress limits of  $\pm 25 \text{ ksi}$ . The nodes are subject to the displacement limits of  $0.25 \text{ in}$ . The members of this truss are categorized 16 groups: (1)  $A_1-A_4$ , (2)  $A_5-A_{12}$ , (3)  $A_{13}-A_{16}$ , (4)  $A_{17}-A_{18}$ , (5)  $A_{19}-A_{22}$ , (6)  $A_{23}-A_{30}$ , (7)  $A_{31}-A_{34}$ , (8)  $A_{35}-A_{36}$ , (9)  $A_{37}-A_{40}$ , (10)  $A_{41}-A_{48}$ , (11)  $A_{49}-A_{52}$ , (12)  $A_{53}-A_{54}$ , (13)  $A_{55}-A_{58}$ , (14)  $A_{59}-A_{66}$ , (15)  $A_{67}-A_{70}$ , and (16)  $A_{71}-A_{72}$ . Table 10 lists the values and directions of the two independent load conditions applied to the 72-bar spatial truss. The cross-sectional areas of truss members are considered as size variables. The sizing variables are chosen from 32 discrete values of  $S = \{0.1, 0.2, 0.3, 0.4, 0.5, 0.6, 0.7, 0.8, 0.9, 1.0, 1.1, 1.2, 1.3, 1.4, 1.5, 1.6, 1.7, 1.8, 1.9, 2.0, 2.1, 2.2, 2.3, 2.4, 2.5, 2.6, 2.7, 2.8, 2.9, 3.0, 3.1, 3.2\} \text{ in}^2$  [8.16]. The present or absent of truss members are selected as topology variables. Fig. 20 illustrates the solution topology obtained by the PSOSCALF. The PSOSCALF evolution process is started at  $W \sim 726.4741 \text{ lb}$  in the first iteration, and converged to  $W \sim 378.3682 \text{ lb}$  after 1000 iterations. The convergence diagram for the best results is shown in Fig. 21. This configuration shows that all constraints of the problem evaluated at the optimum results by the PSOSCALF are satisfied. In this problem, the population size and the maximum iteration are equal to 80 and 1000, respectively. Fig. 22 compares the existing and permissible displacement and stress values for the optimized 72-bar truss using the PSOSCALF method, ensuring compliance with design constraints. Also, subfigures (a), (b), and (c): Show nodal displacements in X, Y, and Z directions. Subfigure (d): Compares stress values in truss members. All stresses remain within safe limits, ensuring structural integrity. The PSOSCALF method successfully optimizes the 72-bar truss while meeting all displacement and stress constraints, achieving a structurally sound and weight-efficient design. The results of solving this problem by the proposed PSOSCALF algorithm and other algorithms are presented in Table 11. According to the result of the PSOSCALF algorithm in Table 11, the elements 13-18 for group 3, the elements 17 and 18 from group 4, the elements 31-34 from group 7, the elements 35 and 36 form group 8, the elements 49-52 for group 11, and the elements 53 and 54 from group 12 are removed from the base structure. Table 11 illustrates the results obtained by all optimization algorithms. The results signify that the MFO, HHO, WOA, WCA, TLBO, RPSOLF, AGPSO and PSOSCALF algorithms design the optimum weight of  $W \sim 395.21 \text{ lb}$ ,  $W \sim 424.55 \text{ lb}$ ,  $W \sim 393.89 \text{ lb}$ ,  $W \sim 381 \text{ lb}$ ,  $W \sim 380.72 \text{ lb}$ ,  $W \sim 406.58 \text{ lb}$ ,  $W \sim 384.60 \text{ lb}$  and  $W \sim 378.36 \text{ lb}$ , respectively. The outcomes illustrate the performance of the PSOSCALF method to solve this issue.

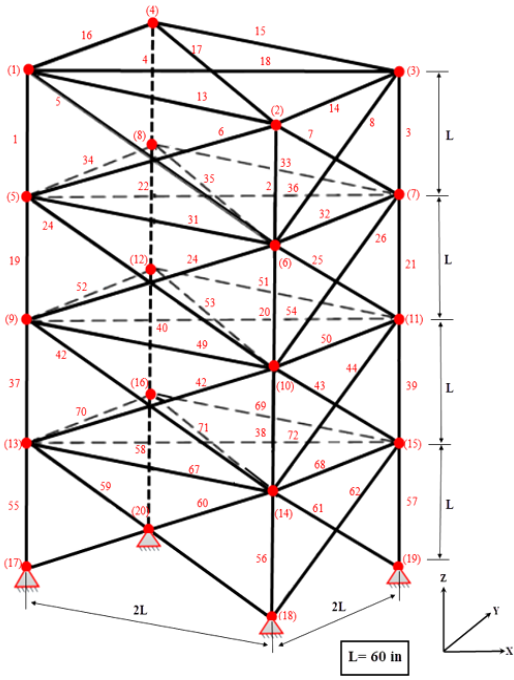


Fig 19 The base structure of the 72-bar spatial truss

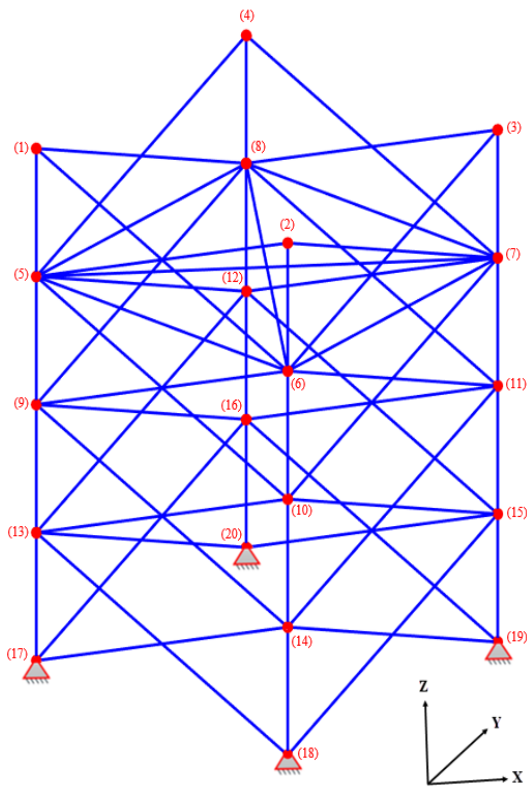
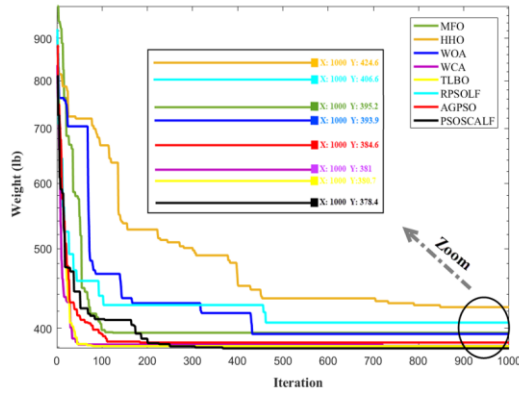


Fig 20 Optimized size and topology 72- bar truss obtained by PSOSCALF



**Fig. 21** Convergence diagram for optimizing 72-bar space truss Size and topology (X= Max iteration Y= Cost value)

**Table 9** Optimal designs for the 25-bar space truss.

Design variables $A_i$ ( $in^2$ ) & $\xi_i$ ( $in$ )	MFO	HHO	WOA	WCA	TLBO	RPSOLF	AGPSO	PSOSCALF
$A_1$	Removed	0.9	0.5	0.1	0.1	0.1	Removed	<b>0.1</b>
$A_2$	0.1	0.3	0.4	0.2	0.1	0.3	0.1	<b>0.1</b>
$A_3$	1.0	0.8	0.7	0.9	1.0	1.4	1.0	<b>0.9</b>
$A_4$	Removed	0.1	Removed	Removed	Removed	Removed	Removed	<b>Removed</b>
$A_5$	0.2	Removed	Removed	Removed	Removed	0.2	Removed	<b>Removed</b>
$A_6$	0.1	0.1	0.2	0.1	0.1	0.1	0.1	<b>0.1</b>
$A_7$	0.1	0.3	0.2	0.2	0.2	0.2	0.1	<b>0.2</b>
$A_8$	1.0	0.9	0.9	0.9	0.9	1.5	1.0	<b>0.9</b>
Shape variables ( $in$ )								
$X_4$	36.8398	20.8110	20	29.5807	33.5968	20	38.6208	<b>33.2843</b>
$Y_4$	80	54.2636	56.6133	63.6720	51.2486	58.8516	58.7214	<b>64.4336</b>
$Z_4$	90	127.1476	125.7931	114.3999	129.9983	90	119.4431	<b>115.5971</b>
$X_8$	45.8615	40.0025	40	40	43.4583	40	48.5885	<b>43.3854</b>
$Y_8$	140	133.2141	136.1155	136.0506	132.7256	100	132.1803	<b>139.7719</b>
Weight ( $lb$ )	121.9319	134.2295	133.2506	119.6150	118.0741	166.5620	116.7475	<b>115.9406</b>
Max. stress ( $ksi$ )	16.1850	30.4310	22.4920	19.9240	17.1770	15.3650	18.4890	<b>16.7060</b>
Max. displacement ( $in$ )	0.3389	0.3500	0.3500	0.3500	0.3500	0.3478	0.3500	<b>0.3500</b>

**Table 10** Loading conditions for the 72-bar spatial truss

Node	Loading condition 1			Loading condition 2		
	$F_x$ (Kips)	$F_y$ (Kips)	$F_z$ (Kips)	$F_x$ (Kips)	$F_y$ (Kips)	$F_z$ (Kips)
1	5.0	5.0	-5.0	0.0	0.0	-5.0
2	0.0	0.0	0.0	0.0	0.0	-5.0
3	0.0	0.0	0.0	0.0	0.0	-5.0
4	0.0	0.0	0.0	0.0	0.0	-5.0

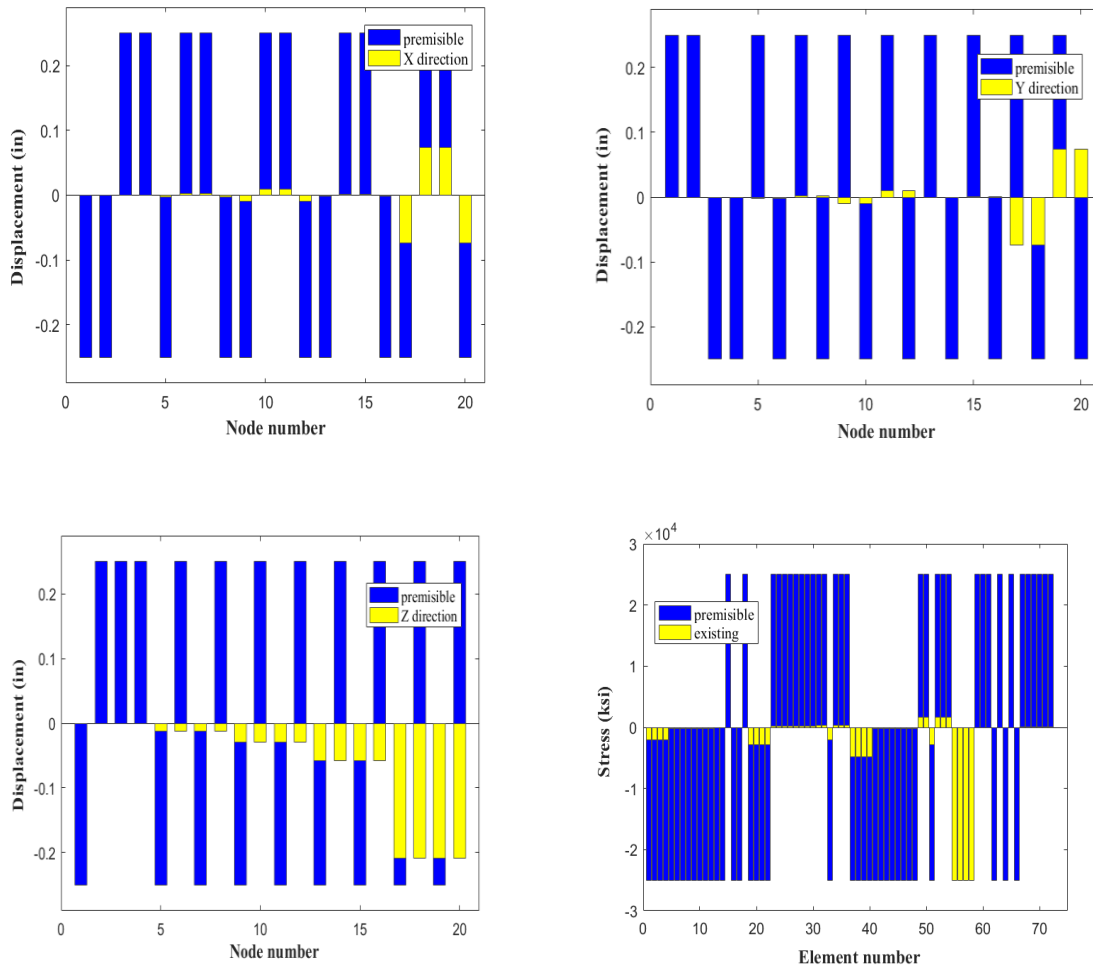


**Fig. 22** Comparison of existing and permissible stresses and displacements for the 72-bar truss by PSOSCALF, (a, b and c) Constraint values of displacement, (d) Constraint values of stress.

### 5.5 The 120-bar Dome Truss

As the last issue in this article, geometric coordinates, as well as the number of nodes and the category of members of a 120-bar dome truss, are shown in Fig. 23. The members of the structure are divided into 7 groups using symmetry, as shown in Fig. 23, [32, 33, 5]. Besides, the permissible tensile and compressive stresses are used according to the AISC 1989 [31] code as follows:

$$\begin{cases} \sigma_i^+ = 0.6F_y & \text{for } \sigma_i > 0 \\ \sigma_i^- & \text{for } \sigma_i < 0 \end{cases} \quad (13)$$

where  $\sigma_i^-$  is calculated according to the slenderness ratio:

$$\sigma_i^b = \begin{cases} \left[ \left( 1 - \frac{\lambda_i^2}{2C_c^2} \right) F_y \right] / \left( \frac{5}{3} + \frac{3\lambda_i}{8C_c} - \frac{\lambda_i^3}{8C_c^3} \right) & \text{for } \lambda_i < C_c \\ \frac{12\pi^2 E}{23\lambda_i^2} & \text{for } \lambda_i \geq C_c \end{cases} \quad (14)$$

**Table 11** Optimal designs for size and topology of the 72-bar spatial truss.

Group number and Design variables $A_i$ ( $in^2$ )	MFO	HHO	WOA	WCA	TLBO	RPSOLF	AGPSO	PSOSCALF
$A_1 - A_4$ (1)	2.9	2.3	32	2.4	2.4	1.7	2.5	<b>2.2</b>
(2) $A_5 - A_{12}$	0.6	0.8	0.5	0.7	0.6	0.9	0.6	<b>0.7</b>
(3) $A_{13} - A_{16}$	Remove d	Remove d	Remove d	Remove d	Remove d	Remove d	Remove d	<b>Removed</b>
(4) $A_{17} - A_{18}$	Remove d	Remove d	Remove d	Remove d	Remove d	Remove d	Remove d	<b>Removed</b>
(5) $A_{19} - A_{22}$	2.5	1.6	3.0	2.0	1.6	1.7	1.9	<b>1.9</b>
(6) $A_{23} - A_{30}$	0.6	1.0	0.8	0.6	0.7	0.7	0.6	<b>0.6</b>
(7) $A_{31} - A_{34}$	0.1	Remove d	Remove d	Remove d	Remove d	Remove d	Remove d	<b>Removed</b>
(8) $A_{35} - A_{36}$	Remove d	0.1	0.1	Remove d	Remove d	Remove d	Remove d	<b>Removed</b>
(9) $A_{37} - A_{40}$	0.8	0.9	0.3	1.1	1.1	0.8	1.1	<b>1.1</b>
(10) $A_{41} - A_{48}$	0.6	0.6	0.8	0.6	0.7	0.9	0.7	<b>0.7</b>
(11) $A_{49} - A_{52}$	Remove d	0.2	Remove d	Remove d	Remove d	Remove d	Remove d	<b>Removed</b>
(12) $A_{53} - A_{54}$	Remove d	Remove d	0.4	Remove d	Remove d	Remove d	Remove d	<b>Removed</b>
(13) $A_{55} - A_{58}$	0.2	0.2	0.3	0.2	0.2	0.2	0.2	<b>0.2</b>
(14) $A_{59} - A_{66}$	1.4	1.5	1.5	1.3	1.3	1.3	1.3	<b>1.3</b>
(15) $A_{67} - A_{70}$	0.6	0.4	0.5	0.6	0.5	0.3	0.6	<b>0.6</b>
(16) $A_{71} - A_{72}$	0.8	0.5	1.1	1.0	1.1	1.2	1.0	<b>0.9</b>
Weight ( $lb$ )	395.21	424.55	393.89	381.00	380.72	406.58	384.60	<b>378.36</b>
Max. stress ( $ksi$ )	25000	25000	16666	25000	25000	25000	25000	<b>25000</b>
Max. displacement ( $in$ )	0.20	0.21	0.19	0.20	0.20	0.22	0.20	<b>0.20</b>

where  $E$  is the modulus of elasticity,  $F_y$  is the yield stress of steel,  $C_c$  divides the elastic and inelastic

buckling regions,  $(C_c = \sqrt{2\pi^2 E / F_y})$ ,  $\lambda_i$  is the slenderness ratio ( $\lambda_i = K_i L_i / r_i$ ),  $k$  is the effective length factor,  $L_i$  is the member length and  $r_i$  is the radius of gyration. In addition, the radius of gyration ( $r_i$ ) can be expressed in terms of cross-sectional areas as  $r_i = aA_i^b$  [34]. The modulus of elasticity is  $E = 30450 \text{ ksi}$ , and the material density is  $\rho = 0.288 \frac{\text{lb}}{\text{in}^3}$ . The yield stress is  $F_y = 58.0 \text{ ksi}$ . Here, the parameters  $a$  and  $b$  are the constants pertaining to the types of sections selected for the members such as pipes, angles, and tees. In this example, pipe sections ( $a = 0.4993$  and  $b = 0.6777$ ) are adopted for bars. The minimum cross-sectional area of all members is  $0.775 \text{ in}^2$ , and the maximum cross-sectional area is taken as  $20.0 \text{ in}^2$ . These loads are taken as  $-13.49 \text{ kips}$  at node 1,  $-6.744 \text{ kips}$  at nodes 2 through 14, and  $-2.248 \text{ kips}$  at the rest of the nodes.

In this example, four cases of constraints are considered as follows:

Case (1): with stress constraints and without any limitations of nodal displacement.

Case (2): with stress constraints and displacement limitations of  $\pm 0.1969 \text{ in}$  are imposed on all nodes in the  $x$  and  $y$ -directions.

Case (3): no stress constraints but displacement limitations of  $\pm 0.1969 \text{ in}$  are imposed on all nodes in the  $z$ -direction.

Case (4): all constraints explained in cases 1, 2 and 3 are considered together.

The convergence diagram of the best results for case 1, case 2, case 3, and case 4 as shown in Fig. 24, 25, 26 and 27, respectively. For all cases, Figs. 28-31 compares the existing values (the member's stresses corresponding to the best solution) and allowable values for stress and displacement constraints. Based on these figures, it can be concluded that the stress and displacement constraints of the structure are not violated and the presented optimum designs are entirely feasible. Also, it can be seen that the axial stresses in most of the members of the structure are very close to the allowable values which show the optimality of the presented designs. In this problem, the population size and the maximum iteration are 50 and 500, respectively. Tables 12, 13, 14 and 15 compare the results obtained for case 1, case 2, case 3, and case 4, respectively. The optimal results of MFO, HHO, WOA, WCA, TLBO, RPSOLF, AGPSO and PSOSCALF algorithms are compared with each other. As you can see, the results of the PSOSCALF algorithm are better than other algorithms in all cases.

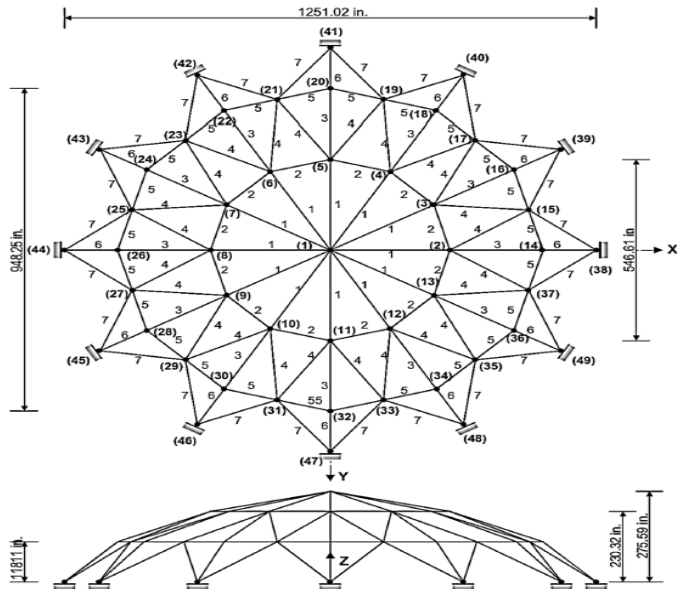


Fig. 23 schematic of the 120-bar dome truss [32].

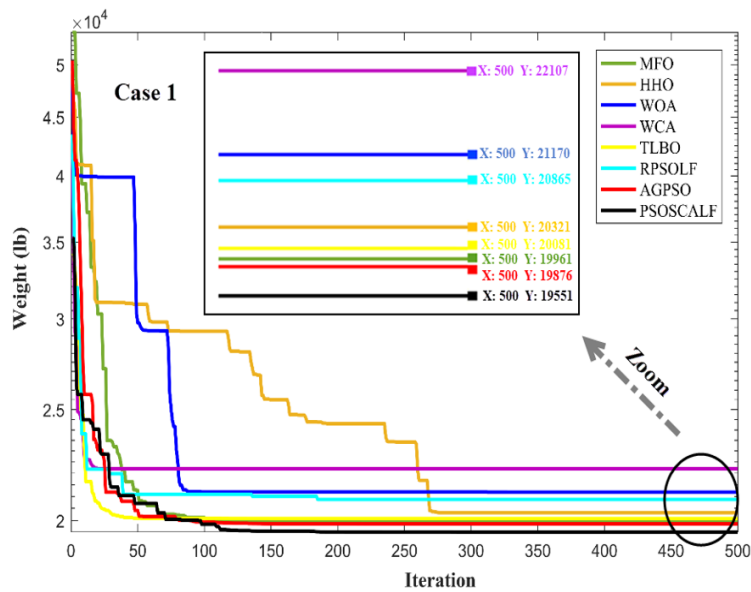
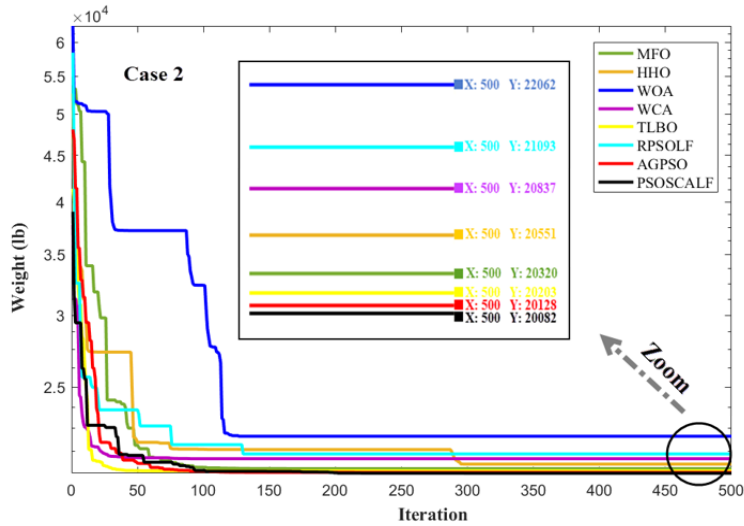
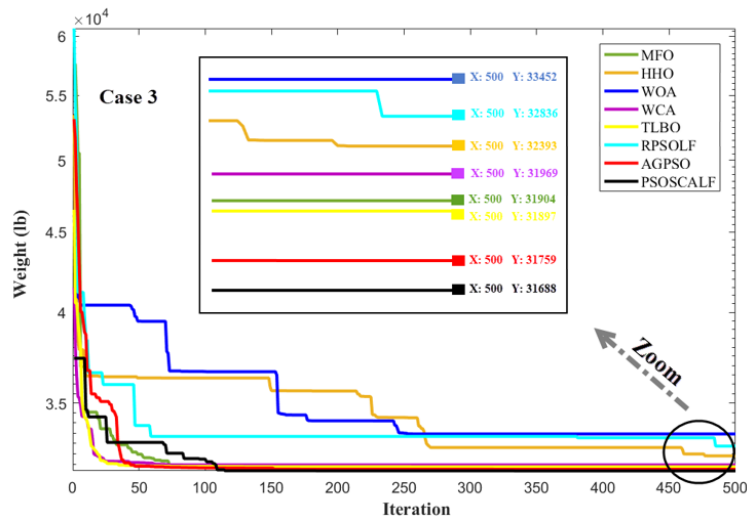


Fig. 24 Convergence diagram for optimizing 120-bar dome space truss Case 1 (X= Max iteration Y= Cost value).



**Fig. 25** Convergence diagram for optimizing 120-bar dome space truss Case 2 (X= Max iteration Y= Cost value).



**Fig. 26** Convergence diagram for optimizing 120-bar dome space truss Case 3 (X= Max iteration Y= Cost value).

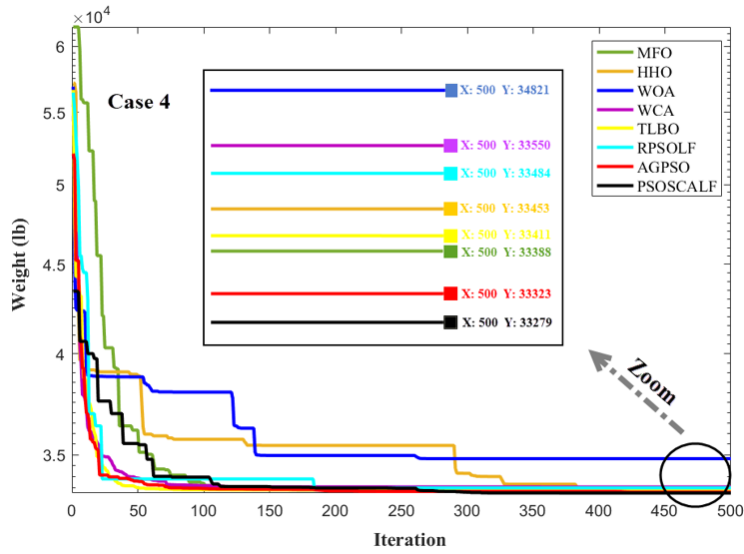


**Fig. 27** Convergence diagram for optimizing 120-bar dome space truss Case 4 (X= Max iteration Y= Cost value).

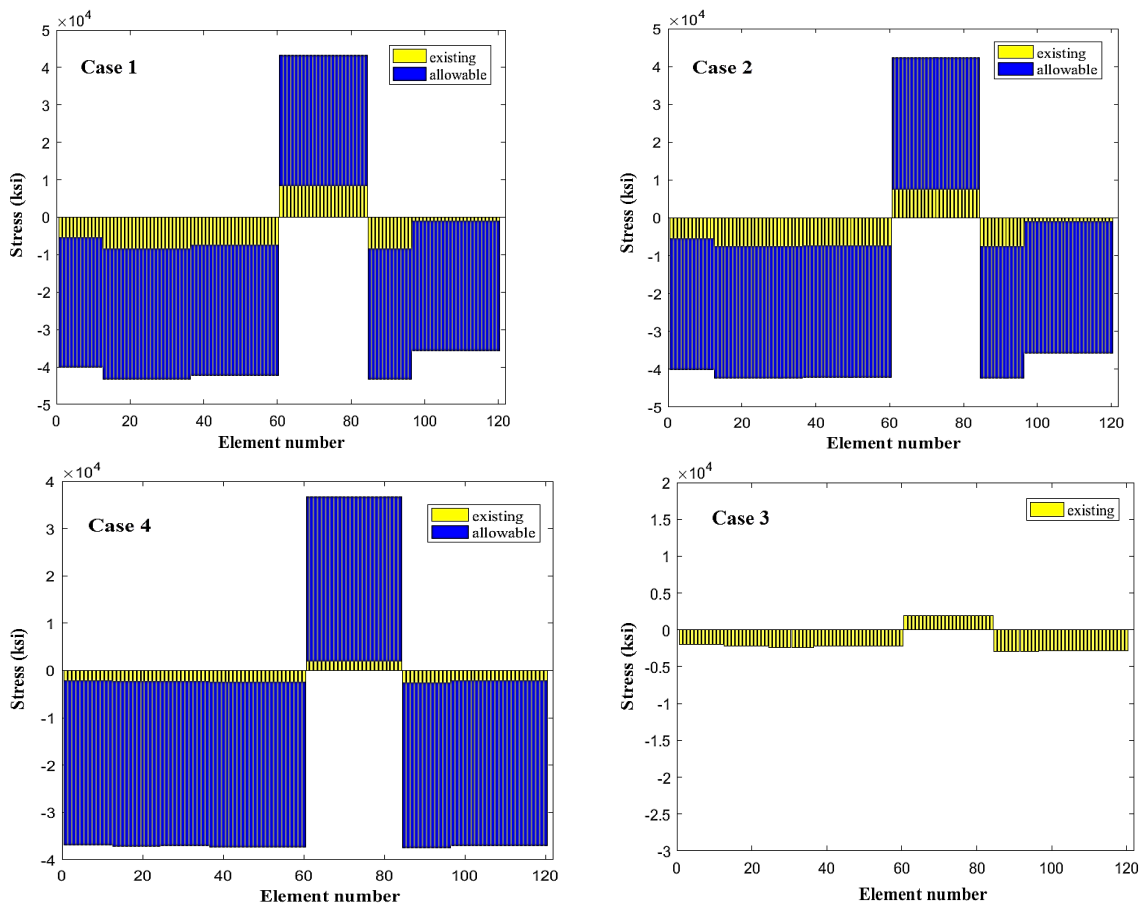


**Fig. 28** Comparison of existing and allowable stresses for the 120-bar dome truss by PSOSCALF (four cases).

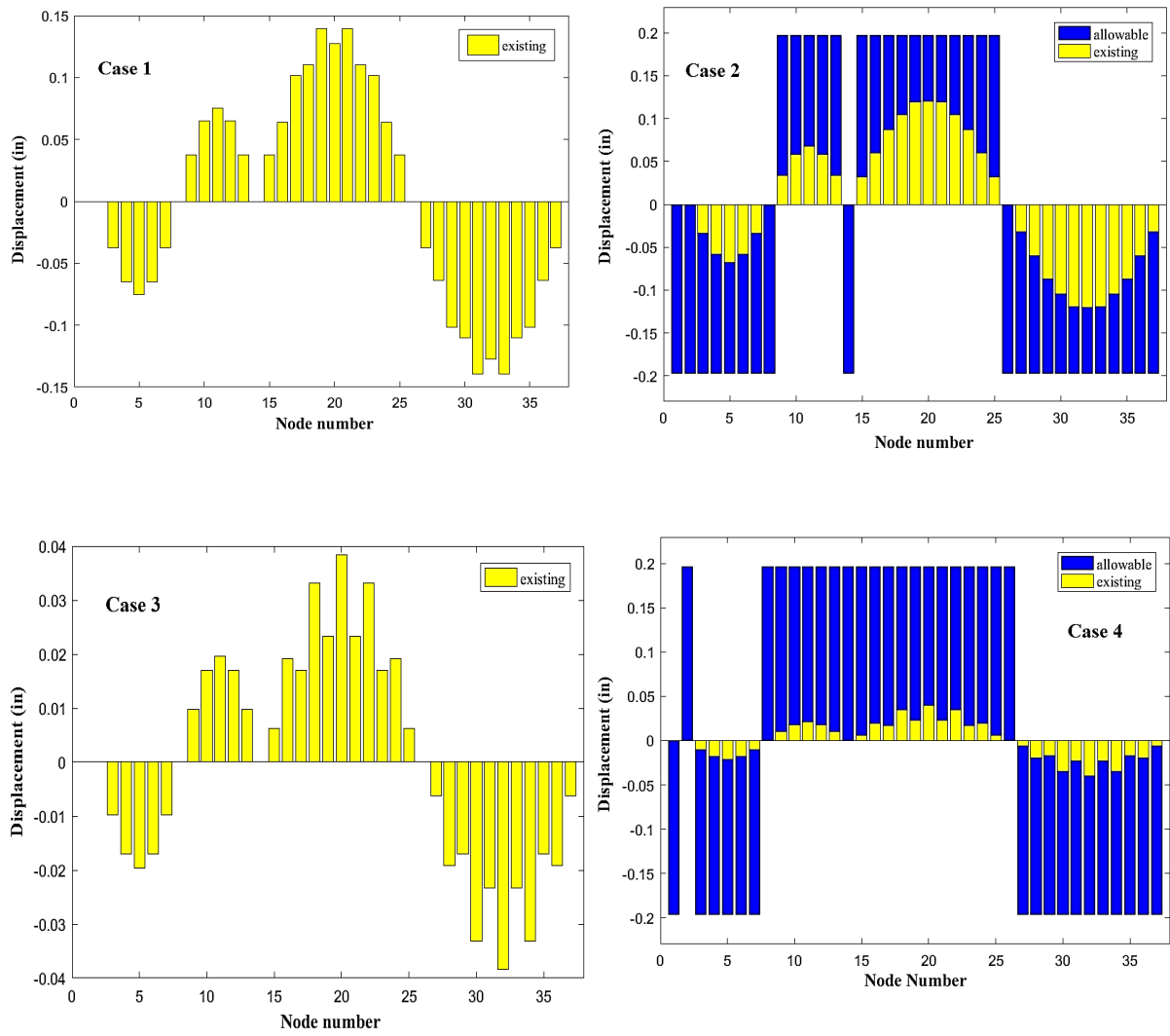


**Fig. 29** Comparison of existing and allowable displacement in the  $x$ -direction for the 120-bar dome truss by PSOSCALF (four cases).

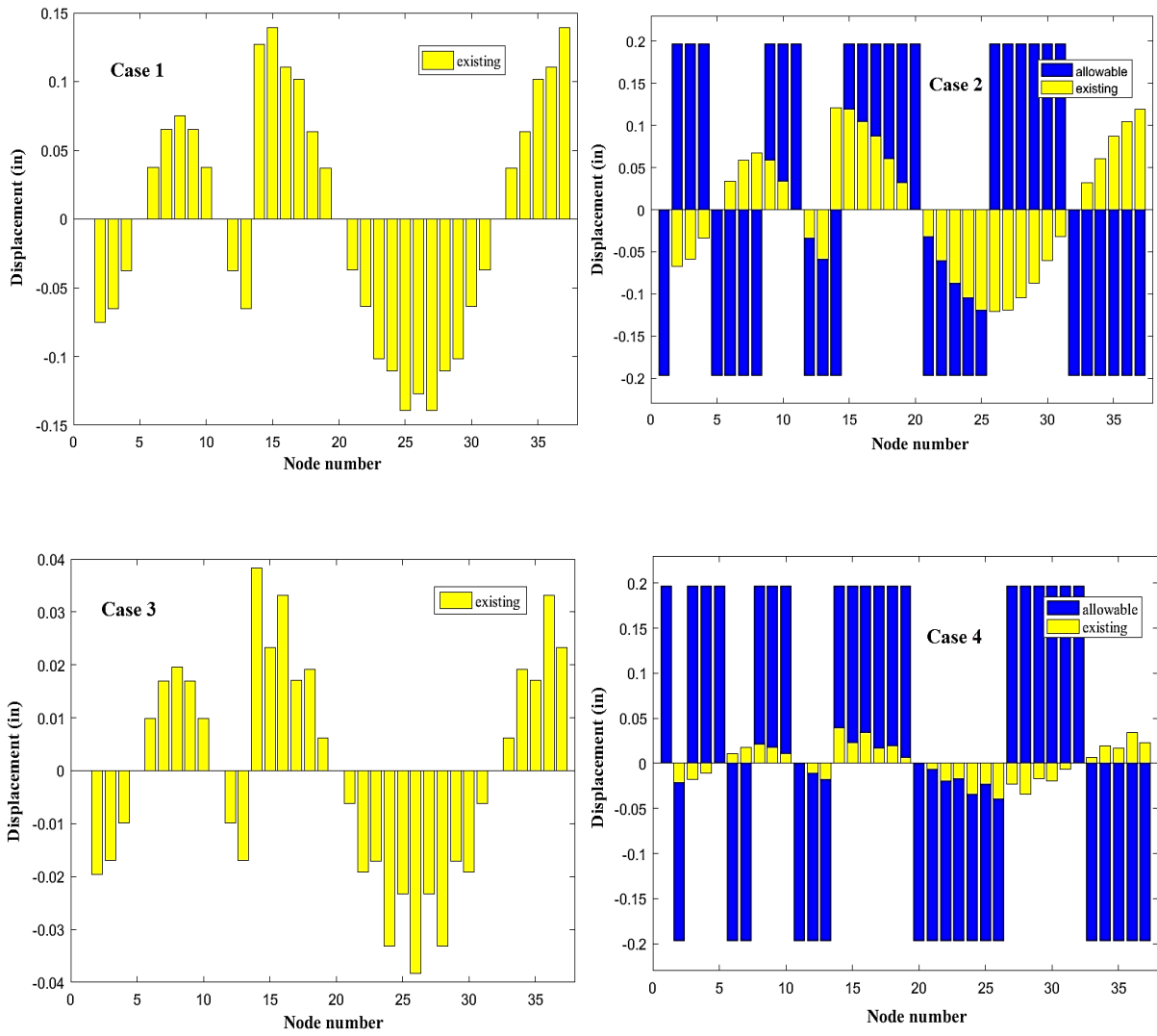


**Fig. 30** Comparison of existing and allowable displacement in y-direction for the 120-bar dome truss by PSOSCALF (four cases).

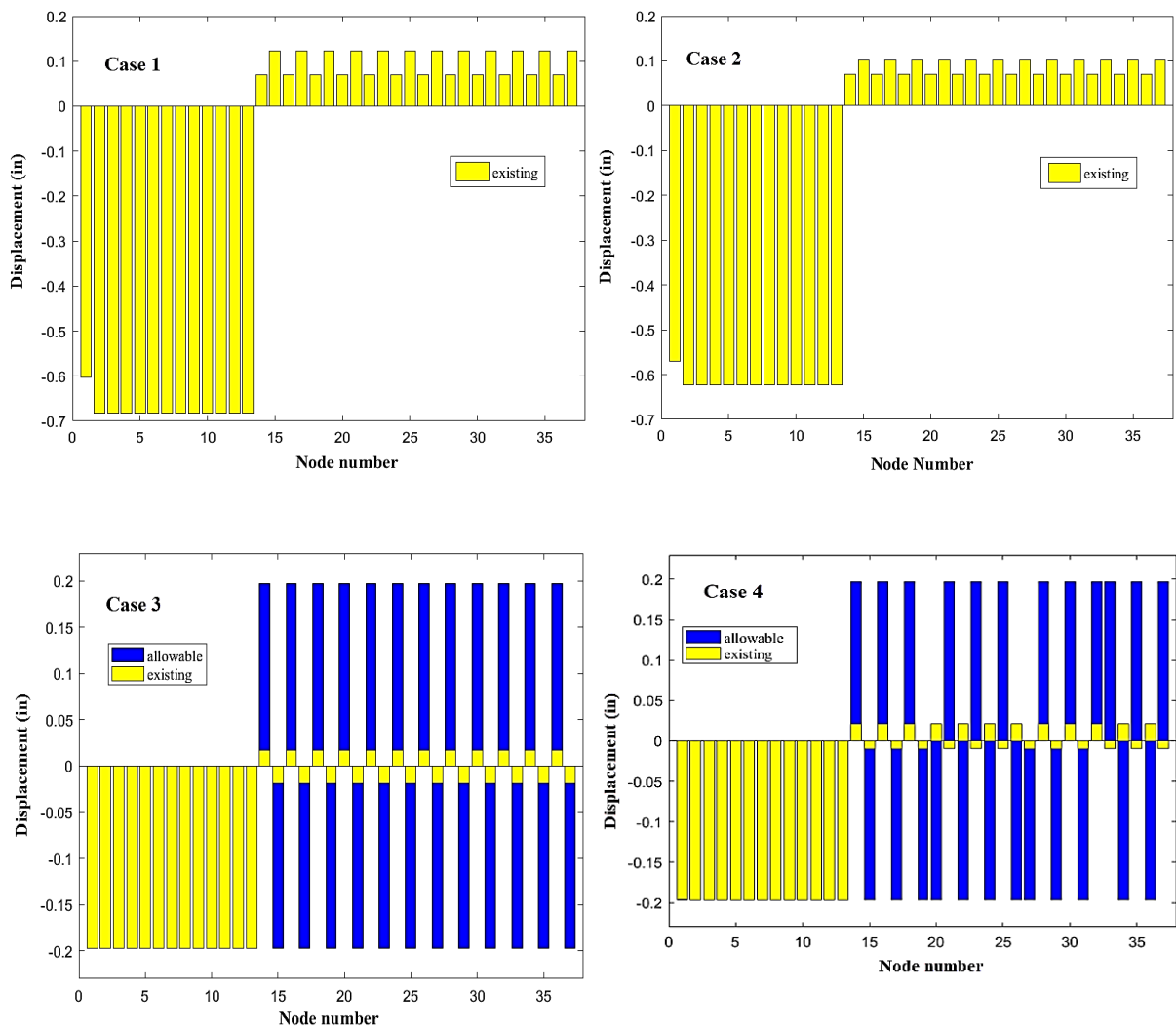


**Fig. 31** Comparison of existing and allowable displacement in z-direction for the 120-bar dome truss by PSOSCALF (four cases)

**Table 12** Optimal results for the 120-bar dome space truss (Case 1)

Element group	MFO	HHO	WOA	WCA	TLBO	RPSOLF	AGPSO	PSOSCALF
<b>Case 1</b>								
$A_1$	0.7550	0.8041	0.7869	0.7550	0.7555	0.7550	0.7550	<b>0.7551</b>
$A_2$	4.3764	3.7918	4.5164	2.5143	4.3744	4.1014	5.0805	<b>3.9649</b>
$A_3$	1.6992	1.4665	3.2246	0.9762	1.6988	1.3038	1.9726	<b>1.5403</b>
$A_4$	0.7550	0.7550	0.7737	0.7550	0.7550	0.7550	0.8522	<b>0.7550</b>
$A_5$	2.3547	2.1925	2.6770	1.3528	2.3535	1.8929	2.7336	<b>2.1324</b>
$A_6$	1.3141	1.1701	1.5224	0.7550	1.3135	1.1897	1.5256	<b>1.1903</b>
$A_7$	5.5816	6.2230	5.4533	8.4048	5.5837	6.8186	4.9993	<b>6.0057</b>
Weight (lb)	19961.42	20321.43	21170.44	22107.31	20081.74	20865.25	19876.45	<b>19551.479</b>
	91	29	90	90	02	22	34	<b>0</b>

**Table 13** Optimal results for the 120-bar dome space truss (Case 2)

Element group Case 2	MFO	HHO	WOA	WCA	TLBO	RPSOLF	AGPSO	PSOSCALF
A <sub>1</sub>	0.7550	0.7554	0.7869	0.7551	0.7550	0.7550	0.7550	<b>0.7563</b>
A <sub>2</sub>	4.4360	4.0162	4.5164	3.7461	4.3276	3.4086	4.6304	<b>4.4150</b>
A <sub>3</sub>	1.7223	1.4665	1.5189	1.4545	1.6804	1.2429	1.7978	<b>1.7139</b>
A <sub>4</sub>	0.7550	0.7550	0.7550	0.7550	0.7550	0.7550	0.7767	<b>0.7550</b>
A <sub>5</sub>	2.3868	2.1925	2.1062	2.0160	2.3288	1.6503	2.4914	<b>2.3751</b>
A <sub>6</sub>	1.3320	1.1701	1.5207	1.1249	1.2995	0.9146	1.3904	<b>1.3261</b>
A <sub>7</sub>	5.5261	6.2230	6.0637	62609	5.6280	7.2981	5.3538	<b>5.5462</b>
Weight (lb)	20320.21	20551.35	22062.28	20837.38	20203.44	21093.46	20128.57	<b>20082.118</b>
	33	52	97	92	42	73	26	<b>4</b>

**Table 14** Optimal results for the 120-bar dome space truss (Case 3)

Element group Case 3	MFO	HHO	WOA	WCA	TLBO	RPSOLF	AGPSO	PSOSCALF
A <sub>1</sub>	1.8665	1.8105	2.0142	2.0437	1.9109	2.0234	1.9095	<b>2.0110</b>
A <sub>2</sub>	14.1162	13.1062	15.2120	15.4651	14.4604	13.0460	14.4497	<b>15.2138</b>
A <sub>3</sub>	5.9207	6.3420	5.0893	5.8699	5.6193	5.8792	5.6765	<b>5.4848</b>
A <sub>4</sub>	2.4920	2.6470	1.8802	2.4125	2.4894	2.0068	2.4942	<b>2.5286</b>
A <sub>5</sub>	9.4776	10.6816	13.6095	9.1656	9.6606	10.6956	9.6272	<b>9.2748</b>
A <sub>6</sub>	3.5739	2.6338	2.3387	3.3307	3.5118	5.2061	3.5141	<b>3.3941</b>
A <sub>7</sub>	2.0292	1.9904	1.9851	1.9260	1.9565	2.2539	1.9444	<b>1.9800</b>
Weight (lb)	31904.23	32393.12	33452.44	31969.04	31897.25	32836.07	31759.59	<b>31688.265</b>
	27	75	93	23	78	32	76	<b>6</b>

**Table 15** Optimal results for the 120-bar dome space truss (Case 4)

Element group Case 4	MFO	HHO	WOA	WCA	TLBO	RPSOLF	AGPSO	PSOSCALF
A <sub>1</sub>	1.7306	1.8975	2.2100	1.8591	1.8392	2.0472	1.7729	<b>1.9115</b>
A <sub>2</sub>	13.0956	13.9974	14.0824	14.0683	13.9153	14.6439	13.4163	<b>14.3710</b>
A <sub>3</sub>	5.8692	5.8380	5.3802	5.3459	5.4616	5.6051	5.5557	<b>5.7562</b>
A <sub>4</sub>	2.5314	2.4278	4.6801	2.4242	2.4161	1.6869	2.4850	<b>2.2709</b>
A <sub>5</sub>	9.4137	8.8566	7.2893	9.3404	9.3538	9.9560	9.5058	<b>9.1056</b>
A <sub>6</sub>	3.9161	4.3752	4.8387	3.9811	4.1786	4.3214	4.0286	<b>3.8241</b>
A <sub>7</sub>	2.4919	2.4144	2.4257	2.4618	2.3758	3.3851	2.4403	<b>2.5448</b>
Weight (lb)	33388.4081	333453.11	1634821.32	8033550.38	9333411.31	5633484.98	9033323.32	<b>5433279.6807</b>

## 6 Conclusions

In the present article, the PSOSCALF algorithm was utilized to SST optimization of truss structures. The PSOSCALF and PSO algorithms were combined together, SCA, and the Levy flight approach.

For investigating the capabilities of the PSOSCALF technique in the SST optimization of trusses, the 2D-truss structures such as the 10-bar truss, the 15-bar truss, and the 18-bar truss and, the 3D-truss structures such as the 25-bar truss, the 72-bar truss and the 120-bar truss were used. In this paper, the structural weight was considered as the objective function and the results of the PSOSCALF algorithm

were compared with the MFO, HHO, WOA, WCA, TLBO, RPSOLF, and AGPSO algorithms. Finally, the outcomes state that:

Comparison of the convergence curves showed that the PSOSCALF optimization algorithm is able to design the 2D and 3D trusses with minimum weight by employing the exploration capability at the beginning of the optimization process and exploitation capability at the final stages of this process. In fact, the optimization results showed that the PSOSCALF technique has a suitable convergence rate in the design of the 2D and 3D trusses.

The optimal design gained via the PSOSCALF algorithm did not violate any of the constraints governing the truss optimization.

In the case of comparing algorithms for optimization of the two-dimensional and three-dimensional trusses, the PSOSCALF optimization is more effective.

### **6.1 Study Limitations**

The fact that the study is based on a specific data set may limit the applicability of the findings in a broader context. However, these limitations may contribute to a more in-depth examination of the topic by providing an essential basis for future research.

### **6.2 Acknowledgments**

This paper is derived from the first author's doctoral thesis.

### **6.3 Funding source**

There is no funding source.

### **6.4 Competing Interests**

There is no conflict of interest in this study.

### **6.5 Authors' Contributions**

All authors approved the final manuscript equally.

## **References**

- [1] S. Rao, *Engineering Optimization Theory and Practice*, John Wiley & Sons 2009.
- [2] B. Auer, *size and shape optimization of frame and truss structures through evolutionary methods*, M.S. thesis Univ. of Idaho 2005.
- [3] Kaveh, S. Talatahari, Particle swarm optimizer, ant colony strategy and harmony search scheme hybridized for optimization of truss structures, *Comput. Struct.* 87 (5-6) (2009) 267–283, <https://doi.org/10.1016/j.compstruc.2009.01.003>.
- [4] C.V. Camp, M. Farshchin, *Design of space trusses using modified teaching-learning based*

- optimization, *Eng. Struct.* 62-63 (2014) 87–97, <https://doi.org/10.1016/j.engstruct.2014.01.020>.
- [5] M. Kooshkbaghi, A. Kaveh, Sizing Optimization of Truss Structures with Continuous Variables by Artificial Coronary Circulation System Algorithm, *IJST-T. CIV. ENG.* 44 (2020) 1–20, <https://doi.org/10.1007/s40996-019-00254-2>.
- [6] M. Cheng, A Hybrid Harmony Search algorithm for discrete sizing optimization of truss structure, *Automat. Constr.* 69 (2016) 21–33, <https://doi.org/10.1016/j.autcon.2016.05.023>.
- [7] H. Assimi, A. Jamali, N. Nariman-zadeh, Sizing and topology optimization of truss structures using genetic programming, *Swarm. Evol. Comput.* 37 (2017) 90–103, <https://doi.org/10.1016/j.swevo.2017.05.009>.
- [8] Y. Wu, Q. Li, Q. Hu, A. Borgart, Size and Topology Optimization for Trusses with Discrete Design Variables by Improved Firefly Algorithm, *Math. probl. eng.* 2017 (2017) 12, <https://doi.org/10.1155/2017/1457297>.
- [9] A. Kaveh, V. Kalatjari, Topology optimization of trusses using genetic algorithm, force method and graph theory *Int. J. Numer. Meth. Eng.* 58 (5) (2003) 771–791, <https://doi.org/10.1002/nme.800>.
- [10] V. Ho-Huu, T. Nguyen-Thoi, M.H. Nguyen-Thoi, L. Le-Anh, An improved constrained differential evolution using discrete variables (D-ICDE) for layout optimization of truss structures, *Expert. Syst. Appl.* 42 (20) (2015) 7057–7069, <https://doi.org/10.1016/j.eswa.2015.04.072>.
- [11] Ahrari, K. Deb, An improved fully stressed design evolution strategy for layout optimization of truss structures, *Comput. Struct.* 164 (2016) 127–144, <https://doi.org/10.1016/j.compstruc.2015.11.00>.
- [12] Ahrari, A.A. Atai, Fully Stressed Design Evolution Strategy for Shape and Size Optimization of Truss Structures, *Comput. Struct.* 123 (2013) 58–67, <https://doi.org/10.1016/j.compstruc.2013.04.013>.
- [13] Mortazavi, V. An, Simultaneous size, shape, and topology optimization of truss structures using integrated particle swarm optimizer, *Struct. Multidisc. Optim.* 54 (4) (2016) 715–736, <https://doi.org/10.1007/s00158-016-1449-7>.
- [14] Ahrari, A.A. Atai, Simultaneous Topology, Shape and Size Optimization of Truss Structures by Fully Stressed Design Based on Evolution Strategy, *Optim. Eng.* 47 (8) (2015) 1063–1084, <https://doi.org/10.1080/0305215X.2014.947972>.
- [15] L.F.F. Miguel, R.H. Lopez, L.F.F. Miguel, Multimodal size, shape, and topology optimization of truss structures using the Firefly algorithm, *Adv. Eng. Softw.* 56 (2013) 23–37, <https://doi.org/10.1016/j.advengsoft.2012.11.006>.
- [16] S.O. Degertekin, L. Lamberti, I.B. Ugur, Discrete sizing/layout/topology optimization of truss structures with an advanced Jaya algorithm, *Appl. Soft. Comput.* 79 (2019) 363–390,

<https://doi.org/10.1016/j.asoc.2019.03.058>.

- [17] S. Nezamivand Chegini, A. Bagheri, F. Najafi, PSOSCALF: A new hybrid PSO based on Sine Cosine Algorithm and Levy flight for solving optimization problems, *Appl. Soft. Comput.* 73 (2018) 697–726, <https://doi.org/10.1016/j.asoc.2018.09.019>.
- [18] S.A. Mirjalili, Moth-flame optimization algorithm: A novel nature-inspired heuristic paradigm, *Knowl. Based. Syst.* 89 (2015) 228–249, <https://doi.org/10.1016/j.knosys.2015.07.006>.
- [19] A.A. Heidari, S. Mirjalili, H. Faris, I. Aljarah, M. Mafarja, H. Chen, Harris hawks optimization: Algorithm and applications, *Future. Gener. Comput. Syst.* 97 (2019) 849–872, <https://doi.org/10.1016/j.future.2019.02.028>.
- [20] S. Mirjalili, A. Lewis, The Whale Optimization Algorithm, *Adv. Eng. Softw.* 95 (2016) 51–67, <https://doi.org/10.1016/j.advengsoft.2016.01.008>.
- [21] H. Eskandar, A. Sadollah, A. Bahreininejad, M. Hamdi, Water cycle algorithm—a novel metaheuristic optimization method for solving constrained engineering optimization problems, *Comput. Struct.* 110–111 (2012) 151–166, <https://doi.org/10.1016/j.compstruc.2012.07.010>.
- [22] R.V. Rao, V.J. Savsani, D.P. Vakharia, teaching–learning-based optimization: A novel method for constrained mechanical design optimization problems, *Comput. Aided. Des.* 43 (3) (2011) 303–315, <https://doi.org/10.1016/j.cad.2010.12.015>.
- [23] B. Yan, Z. Zhao, Y. Zhou, W. Yuan, J. Li, J. Wu, D. Cheng, A particle swarm optimization algorithm with random learning mechanism and levy flight for optimization of atomic clusters, *Comput. Phys. Commun.* 2019 (2017) 79–86, <https://doi.org/10.1016/j.cpc.2017.05.009>.
- [24] S. Mirjalili, A. Lewis, A.S. Sadiq, Autonomous particles groups for particle swarm optimization, *Arab. J. Sci. Eng.* 39 (6) (2014) 4683–4697, <https://doi.org/10.1007/s13369-014-1156-x>.
- [25] Y. Shi, R. Eberhart, A modified particle swarm optimizer, in: *The 1998 IEEE International Conference on Evolutionary Computation Proceedings*, Anchorage, AK, 1998, pp. 69–73.
- [26] K. Deb, S. Gulati, Design of truss-structures for minimum weight using genetic algorithms, *Finite. Elem. Anal. Des.* 37 (5) (2001) 447–465, [https://doi.org/10.1016/S0168-874X\(00\)00057-3](https://doi.org/10.1016/S0168-874X(00)00057-3).
- [27] H. Rahami, A. Kaveh, Y. Gholipour, Sizing, geometry, and topology optimization of trusses via force method and genetic algorithm, *Eng. Struct.* vol. 30 (9) (2008) 86–99, <https://doi.org/10.1016/j.engstruct.2008.01.012>.
- [28] S. Gholizadeh, Layout optimization of truss structures by hybridizing cellular automata and particle swarm optimization, *Comput. Struct.* 125 (2013) 86–99, <https://doi.org/10.1016/j.compstruc.2013.04.024>.
- [29] O. Hasançebi, F. Erbatur, On efficient use of simulated annealing in complex structural optimization problems, *Acta. Mech.* 157 (1-4) (2002) 27–50,

<https://doi.org/10.1007/BF01182153>.

- [30] W. Tang, L. Tong, Y. Gu, Improved genetic algorithm for design optimization of truss structures with sizing, shape and topology variables. *Int. J. Numer. Meth. Engng.* 62 (13) (2005) 1737–1762, <https://doi.org/10.1002/nme.1244>.
- [31] K.S. Lee, Z.W. Geem, A new structural optimization method based on the harmony search algorithm, *Comput. Struct.* 82 (9-10) (2004) 781–798, <https://doi.org/10.1016/j.compstruc.2004.01.002>.
- [32] A. Kaveh, S. Talatahari, Size optimization of space trusses using Big Bang-Big Crunch algorithm. *Comput. Struct.* 87 (17-18) (2009) 1129–1140. <https://doi.org/10.1016/j.compstruc.2009.04.011>.
- [33] AISC-ASD. *Manual of Steel Construction Allowable Stress Design*, 9th Ed. American Institute of Steel Construction, Chicago (IL), USA, 1989.
- [34] M. Saka, Optimum design of pin-jointed steel structures with practical applications, *J. Struct. Eng.* 116 (1990) 2599–2620.